Exhumation of the Peake and Denison Ranges; insights from low-temperature thermochronology

Thesis submitted in accordance with the requirements of the University of Adelaide for an Honours Degree in Geology

James William Hall

November 2014

THE UNIVERSITY of ADELAIDE

EXHUMATION OF THE PEAKE AND DENISON RANGES; INSIGHTS FROM LOW-TEMPERATURE THERMOCHRONOLOGY

EXHUMATION OF THE PEAKE AND DENISON RANGES

ABSTRACT

Multi-method thermochronology applied to the Peake and Denison Ranges (northern South Australia) reveals multiple episodes of exhumation. Apatite Fission Track (AFT) data suggest three time periods in which exhumation induced basement cooling of the Ranges into AFT closure temperatures (~60-120 °C): Approximately 470-440 Ma, 340-290 Ma and 200-180 Ma. The Carboniferous and Jurassic exhumation episodes are supported by additional zircon (ZHe) and apatite (AHe) (U-Th-Sm)/He results respectively. We interpret the first pulses of rapid cooling as a result of the final pulses of the Delamerian and/or start of the Alice Springs Orogeny. Erosion and sedimentary burial during the Devonian brought the basement rocks back to ZHe closure temperatures (~200-180 °C). Shortly after, during the Carboniferous, the Ranges were exhumed to the surface which is likely a result of the final pulse of the Alice Springs Orogeny (~300 Ma). The presence of the Mount Margaret Surface during the Late Permian provides independent geological evidence that the Ranges were exposed at the surface at that time. During the Late Triassic-Early Jurassic, the Ranges were once again reheated to AFT closure temperatures, however, the lack of preserved sedimentary rocks of age suggests that this may not be simply due to burial.

Alternatively, the Ranges could have been affected by a well-documented and widespread hydrothermal pulse, which reheated the rocks without significant sedimentary burial. Cretaceous AHe ages coupled with the presence of coarse-grained terrigeneous rocks at that time indicate that the ranges were shallowly buried during this time before Late Cretaceous exhumation (potentially caused by the rifting of Antarctica from Australia), exhumed the Ranges back to the surface. One additional Miocene AHe age was obtained near the fault-escarpment of the Davenport Range. This was thought to be related with enhanced fault activity at that time and finalised the exhumation history of the Ranges.

KEYWORDS

Exhumation, Peake and Denison Ranges, Low-Temperature Thermochronology, Apatite Fission Track, Apatite Helium, Zircon Helium, South Australia.

TABLE OF CONTENTS

LIST OF FIGURES AND TABLES

INTRODUCTION

The Peake and Denison Ranges are located in the north eastern region of the Gawler Craton. They are dominated by Proterozoic sedimentary and metamorphic rocks with abundant Paleoproterozoic to Ordovician igneous intrusive and extrusive rocks (Ambrose *et al.* 1981). There are three significant igneous bodies in the Ranges; the Tidnamurkuna Volcanics, the Wirriecurrie Granite and the Bungadillina Monzonite (Hopper 2001). While the formation of the Peake and Denison Ranges has been well studied (Ambrose *et al*. 1981; Morrison 1989; Hopper 2001), to date no comprehensive low-temperature thermochronological study has been conducted on the Ranges to determine the timing of exhumation to shallow crustal levels. The exhumation history has been inferred from regional detrital zircon studies such as MacDonald *et al*. (2013) which theorised regional exhumation in the Gawler Craton to be Mid Cretaceous. However, two pilot low-temperature thermochronological and structural studies on the exhumation history have determined different timings for the exhumation for the Peake and Denison Ranges (Wopfner 1968; Radke 1973). These studies reported Permian (266 ±23 Ma) Apatite Fission Track ages for the Bungadillina Monzonite intrusion and Miocene to Pleistocene exhumation ages based on gypsite surfaces across the Levi Fault (Figure 2).

This thesis aims to provide a more rigorous and detailed model for the low-temperature exhumation of the Peake and Denison Ranges. It will determine if, contrary to previous studies, the Delamerian and Alice Springs Orogenies were the main mechanisms for exhumation in the region, and if later Mesozoic exhumation occurred as a result of prolonged regional tectonic activity (proposed by MacDonald *et al*.; 2013) followed by a period of fault-reactivation and associated denudation during the Miocene and

Pleistocene, proposed by Wopfner (1968). This is significant as this will allow the exhumation of the Peake and Denison Ranges and northern South Australia as a whole to be linked with other exhumation studies in South Australia e.g. south and eastern Gawler Craton (Reddy Hons. thesis 2014), and the Flinders Ranges (Foster *et al*. 1994; Mitchell *et al*. 2002; Weisheit *et al*. 2014), This thesis fits into a larger project to characterise and understand the low temperature exhumation history of South Australia. In order to provide models on the low-temperature thermal history of the Peake and Denison Ranges, Apatite Fission Track (AFT) analysis (using the laser-ablation inductively coupled plasma mass spectrometry (LA-ICP-MS) method) was applied to model the exhumation history of the Ranges below 120 °C. Additional apatite (U-Th-Sm)/He (AHe) dating and zircon (U-Th-Sm)/He (ZHe) dating was conducted on selected samples, with the intention of refining the exhumation history model of the Ranges between approximately 75-45 °C and 200-170 °C respectively (Farley 2002; Reiners *et al*. 2004). By combining these methods, a permissive model of the exhumation history is postulated. This model is linked with the sedimentological record of the adjacent basins and possible tectonic events are discussed that may have caused the exhumation of the Peake and Denison Ranges.

GEOLOGICAL SETTING

The Peake and Denison Ranges are comprised of Mesoproterozoic metamorphic rocks, Neoproterozoic sedimentary rocks and Paleoproterozoic to Ordovician igneous intrusive and extrusive rocks (Ambrose *et al*. 1981). The surrounding landscape is covered by Cretaceous sedimentary rocks and Miocene to Pleistocene sediments of the Lake Eyre Basin (Figure 2). The main igneous bodies in the study area are the Wirriecurrie Granite, the Tidnamurkuna Volcanics and the Bungadillina Monzonite. The

Wirriecurrie Granite is of Paleoproterozoic age (1793 ± 8 Ma for Wirriecurrie Granite using U-Pb SHRIMP dating by Rogers and Freeman; 1994) and is deformed towards its margins. There are two deformation events recorded in the Wirriecurrie Granite, which are thought to be related to the Musgravian and Delamerian Orogenies (evidenced by Musgravian and Delamerian K-Ar ages; Ambrose *et al*. 1981). The Tidnamurkuna Volcanics are Paleoproterozoic (1806 ± 27 Ma; Fanning *et al*. 1988) basaltic dominated flows with two episodes of rhyolitic flows. The Bungadillina Monzonite is the name given to a series of monzonites, syenites and gabbros. Their intrusion is the result of the Delamerian Orogeny and they have been dated to be Ordovician in age (497.5 ± 10 Ma using U-Pb; Rogers and Freeman 1994). Additional lamprophyre and dolerite dykes are associated with the Bungadillina Monzonite and were also formed during the same event.

After the formation of the Bungaillina Monzonite, a series of sedimentary rocks were deposited within the region. The first sedimentary rock preserved is the Nultaddy Seismic Unit which is a poorly studied shale unit deposited during the Devonian (Allender *et al*. 1987). This unit is unconformably overlain by the Late Carboniferous to Early Permian, Arckaringa Basin sediments (Boorthanna, Stuart Range, and Mount Toondina Formations) that were deposited as alternating shales and sandstone layers with coal layers present near the top. The presence of coal layers indicates that these are terrestrial deposits. An erosional peneplain known as the Mount Margaret Surface (MMS) is located on the Davenport Range (Figure 2) and has been documented to be late Permian in age (Rogers and Freeman 1994). This demonstrates that the Ranges were at the surface during this time. There are no recorded sedimentary rocks from the

Early Permian until the late Jurassic, when the medium to coarse grained Algebuckina Sandstone was deposited.

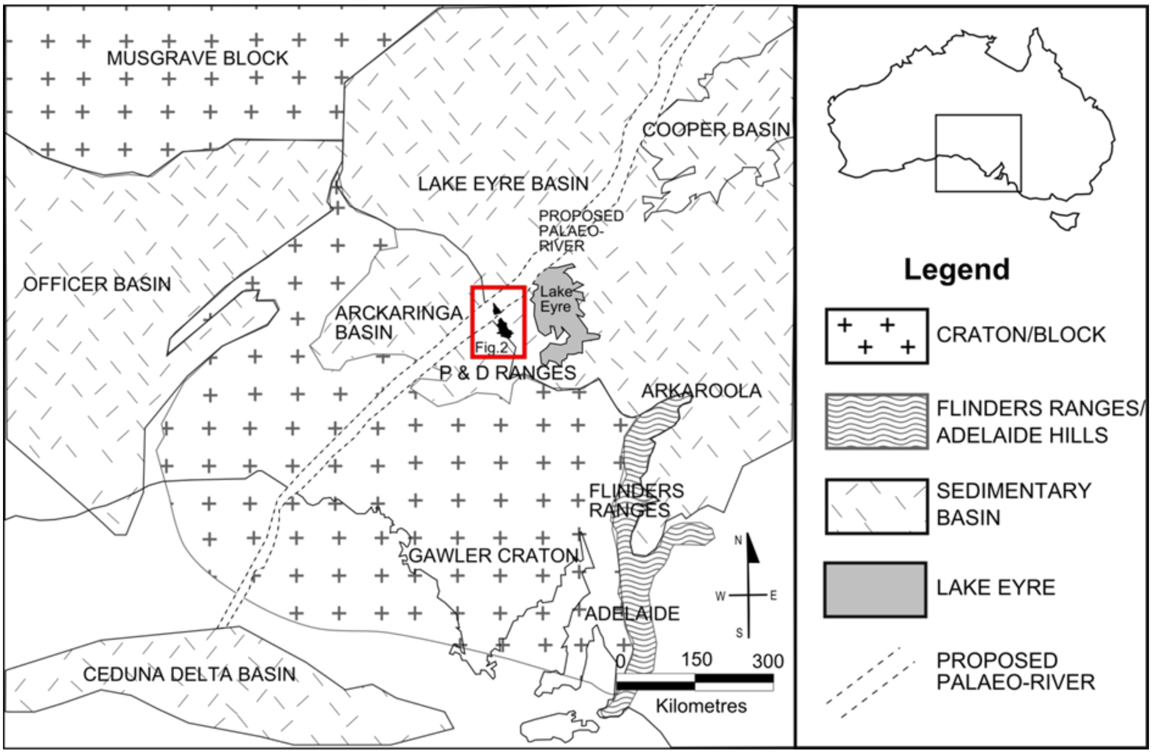

Figure 1, simplified map of South Australia illustrating the outlines of the main geological units: the Gawler Craton, Musgrave Block, Flinders Ranges, and the main sedimentary basins: Officer Basin, Arckaringa Basin, Lake Eyre Basin and Cooper Basin. The Peake and Denison Ranges are indicated in black and are located at the margin between the Lake Eyre and Arckaringa Basins. The locations of the Ceduna Basin and the proposed palaeo-river are plotted as well (after MacDonald *et al.*; 2013) to illuminate the relationship between the proposed river system and the Peake and Denison Ranges (see text for further discussion).

The top of this sandstone unit is silicified and contains plant fossils, which is indicative of a terrestrial origin. Following a short intermission, deposition reoccurred during the Early Cretaceous with the deposition of the Neales River Group sediments. The Mt. Anna Sandstone Member, Cadna-Owie Formation, Bulldog Shale, Coorikiana Sandstone, and Oodnadatta Formation make up this group. These units are made up of alternating shales and sandstones within each unit. Cenozoic deposition consists of mostly coarse terrestrial units including the Mirackina Conglomerate, which is a palaeochannel deposit, as well as unnamed conglomerates, gravels, alluvial deposits, clay deposits, and aeolian sands at the top. These sedimentary units were largely deposited in the Late Eocene – Early Pliocene and Pleistocene – Holocene.

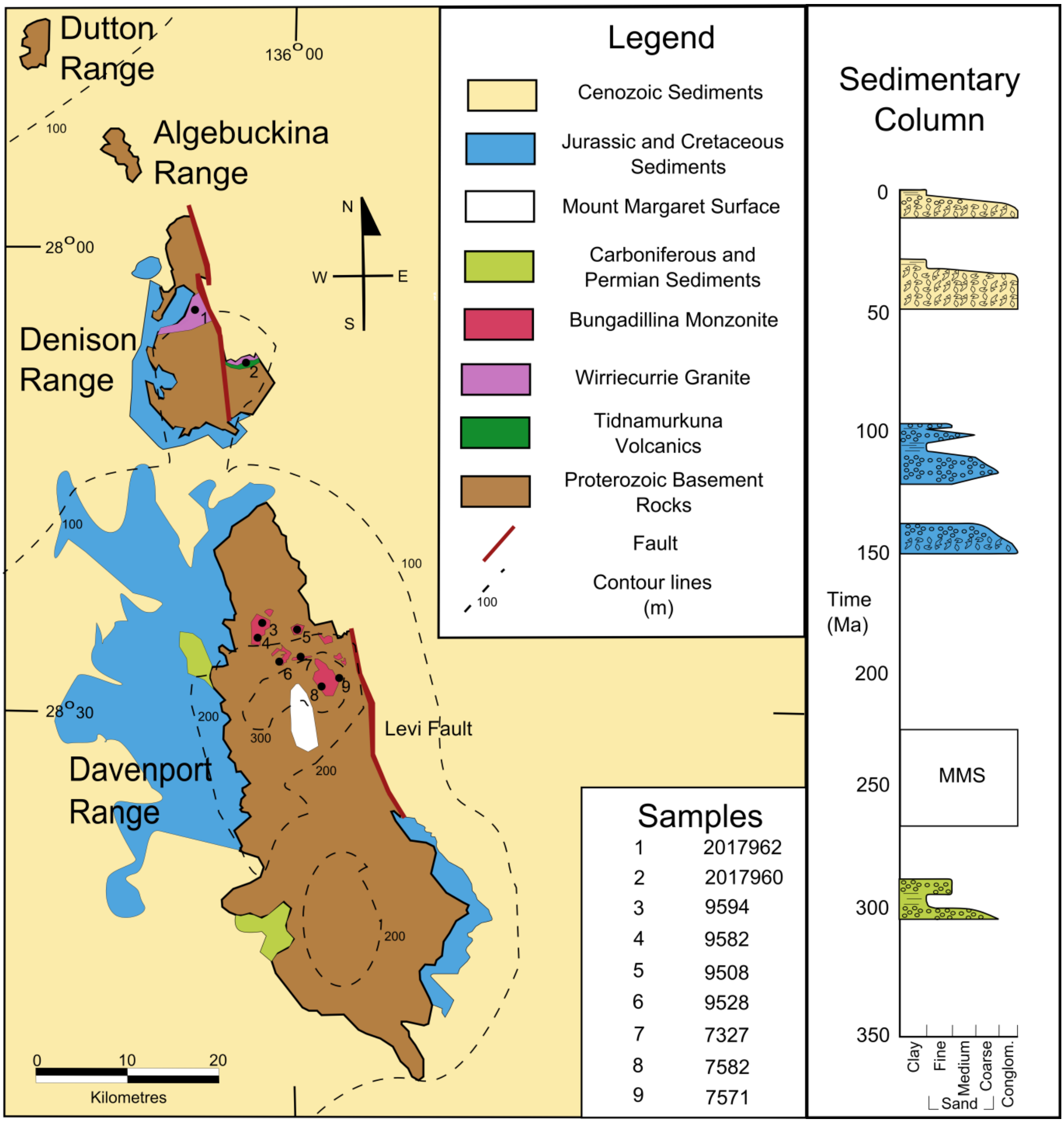

Figure 2, Simplified geological map and stratigraphic column of the Peake and Denison Ranges, indicating the relationship between and ages of different geological units, the location of major faults, topographic contour lines and sample localities. Samples 2017962 and 2017960 were collected and supplied by the Geological Survey of South Australia (Fanning *et al.* 2007). All other samples were collected by University of Adelaide PhD Candidate, Morrison (1989) and supplied by Prof. John Foden. Map modified after Hopper (2001).

In addition to the older deformation events as a result of the Musgravian and Delamerian Orogenies there have been three major tectonic events documented in the vicinity of the study area since the Delamerian Orogeny which may have induced exhumation of the Ranges. Radke (1973) obtained AFT data suggesting an exhumation event during the Permian (266 ± 23 Ma). Additionally, various papers (Twidale 1994; Kohn *et al*. 2002; MacDonald *et al*. 2013) report widespread exhumation in the Gawler Craton during the Upper Cretaceous, therefore it is highly plausible this exhumation also affected the Peake and Denison Ranges. The final tectonic event suggests there was uplift and faulting during the Miocene and Pleistocene, which is recorded by the displacement of morphological features such as gypsite surfaces (Wopfner 1968) across the Levi Fault in the region. This is supported by Foster *et al*. (1994) who concluded that there was exhumation during the Miocene in the northern Flinders Ranges. Waclawik *et al*. (2008) and Reynolds *et al*. (2006) show evidence (deformation of Miocene sediments and intra-cratonic stresses) for neo-tectonism in the region which supports this theory of recent exhumation of the Ranges.

Any major tectonic uplift events that induced exhumation of the Peake and Denison Ranges will have proximal and distal effects on surrounding sedimentary basins as well. The Arckaringa Basin’s eastern margin is at the base of the Peake and Denison Ranges while the Lake Eyre Basin sits on the Ranges eastern margin (Figure 1). Wopfner (1964) showed that exhumation of the ranges had caused faulting in the nearby basins. More recently, MacDonald *et al*. (2013) theorised that the Ceduna River flowed over the Peake and Denison region during the Cenomanian. This theory implies that the Peake and Denison Ranges were not topographic highs at that time unless they served as secondary sedimentary source regions for the Ceduna delta sediments. If the Ranges had been exhumed on the other hand, they would serve as a boundary and thus prevent flow to the south. Hence, unravelling the exhumation history of the Peake and Denison Ranges is paramount to understand the landscape evolution of northern South Australia as well as important to evaluate source-to-sink models for the offshore Ceduna Delta Basin.

METHODOLOGY

Granitoid rock samples were taken from outcrops at the Peake and Denison Ranges by Morrison (1989) and by researchers of the Geological Survey of South Australia (Fanning *et al*. 2007). The Morrison (1989) samples were received as whole-rock samples, while the Fanning *et al*. (2007) samples were provided by Dr. Anthony Reid as apatite and zircon mineral separates. Rock crushing was completed using conventional crushing methods after which, the crushed rock underwent separation via panning, the magnetic separation and conventional heavy liquid separation. Apatite grains were picked out from these separates and mounted in resin on a slide, after which they were ground down and polished. After sufficient polishing they were etched with 20 °C, 5 M HNO_3 for 20 seconds. This etching process reveals the fission tracks in apatite and allows the fission tracks to be counted under a microscope. The counting process was completed in a reference grid raster under an Olympus BX51 Microscope at 1000x magnification. Confined tracks, fission track etch pits (D_{par}) and the angles of the confined tracks to C-axis were measured using an Olympus DP21 camera and computer attachment. These were recorded to estimate the rate of cooling through the AFT closure temperature. The concentrations of U^{238}, U^{235} and Ca^{44} on each grain were determined using a Laser-Ablation Inductively-Coupled-Plasma Mass-spectrometer (LA ICP MS) at Adelaide Microscopy (Resonetics laser system coupled with an

Argilent 7700s quadruple mass spectrometer). The LA ICP MS precisely measured the concentrations of the U^{235}, U^{238}, and Ca^{44} isotopes, which are required to calculate the AFT age of each analysed grain. The concentrations were measured from the exact spot where the fission tracks were counted as the concentration of U and Ca is often variable within the apatite grain (Hasebe *et al*. 2004). Calibration of the LA ICP MS was carried out against a suite of NIST glass standards and using Durango apatite as secondary standard. Ca^{44} was used as an internal standard. Data reduction was carried out using in-house Excel spreadsheets. A minimal amount of unreliable U-concentrations (mainly due to heavily zoned U-concentrations) were not used further in the AFT age calculations.

Two apatite and one zircon separate were chosen based on grain quality to be sent to the John De Laeter Centre at Curtin University for (U-Th-Sm)/He dating. He-gas was extracted from these grains using a Nd-YAG laser before they were digested in acid. Finally, the U, Th, and Sm concentration of the samples was recorded using an Agilent 7500CS mass spectrometer.

AFT age results, length distributions and (U-Th-Sm)/He age results were subsequently modelled using the *HeFTy* software (Ketcham 2005), to constrain the simulated thermal history evolution of the study region between ~200 °C and surface outcrop temperatures. Multiple age-components were identified using the automatic mixture model in the *Radial Plotter* Software (Vermeesch 2009), which are discussed further below.

RESULTS

Calibration procedures

AFT analysis was the main method applied in this thesis to deduct the low-temperature thermal history of the Peake and Denison Ranges. In order to validate the results presented in this thesis, which was obtained by a novel analytical protocol described in the attached supplementary files, an accuracy check was performed on Durango apatite standard and an in-house apatite standard (ARK 717) from Arkaroola (coordinates 341962E, 6657785N, GDA94). Durango apatite is a well-known standard in the fission track community and was precisely dated with the ^{40}Ar-^{39}Ar method as 31.44 ± 0.18 Ma (McDowell *et al*. 2005).

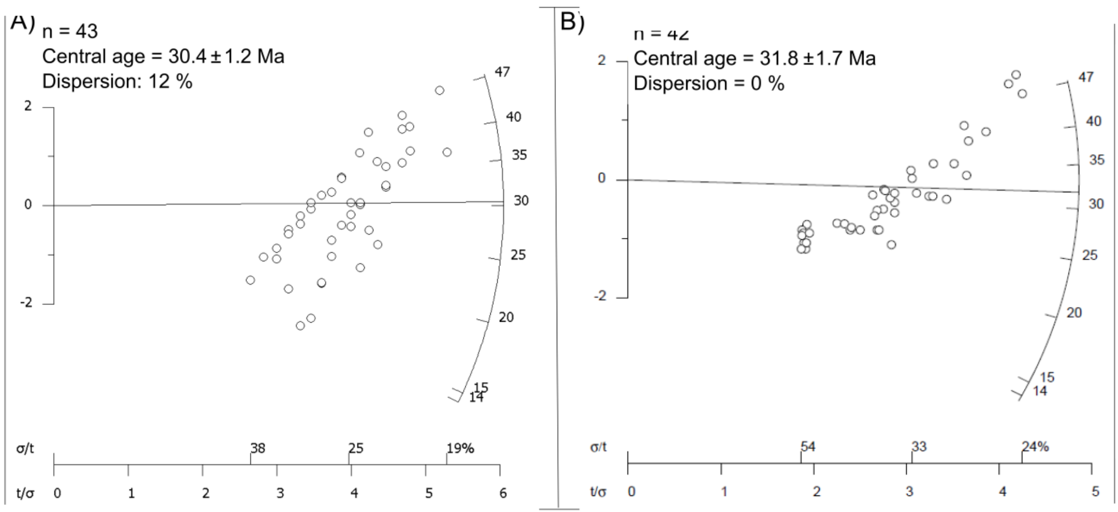

Figure 3, a, Radial plot of Apatite Fission Track (AFT) ages of the Durango standard, from this thesis, using the laser ablation-inductively coupled plasma-mass spectrometer (LA-ICP-MS) method indicating the degree of dispersion, central age, and number (n) of samples counted. In the radial plot, each analysed age is plotted against its precision, which is used to distinguish potential multiple age-components. The obtained central age of 30.4 ± 1.2 Ma is within error of the standard Durango age of 31.44 ± 0.18 Ma old (McDowell *et al*. 2005). b, Radial plot of AFT ages from De Grave *et al*. (2012) using the same method protocol. As shown, similar central ages and data-trends were obtained. These central ages are in good agreement with the precisely obtained age (McDowell *et al*. 2005). Individual apatite AFT ages are displayed by running a straight line from the left of the plot, starting at the 0 point, through the grain, to the right side which reveals the age (in Ma). As the standard deviation is on the x-axis, the age of the samples are more precise if they are plotted closer to the right side of the plot. The error bar is shown as ± 2 σ on the left which is identical for all the grains. The radial plots were constructed using *Radial Plotter* (Vermeesch 2009).

Since this standard apatite is sourced from an immediately cooled volcanic tuff, all other thermochronometers should report the exact same age. A total of 43 Durango analyses were carried out during this thesis, resulting in an overall mean AFT age of 30.4 ± 1.2 Ma (Figure 3). This is within error of the precisely obtained ^{40}Ar-^{39}Ar age of 31.44 ± 0.18 Ma (McDowell *et al*. 2005). These AFT ages were compared to Durango AFT ages collected by De Grave *et al*. (2012) using the same protocol in a different lab to indicate the validity of the protocol.

Figure 4 shows the results obtained for in-house standard ARK 717. The results obtained in this study (Figure 4, panel c) are compared with analyses by 2014 Honours student Jack Gillespie (Figure 4, panel b), which used the same analytical protocol, and with unpublished data from Dr. Stijn Glorie on a sample from the same region (TTN-1) using the classical AFT method (Ghent, Belgium). As shown, the intra-laboratory results are highly comparable (117 ± 6 Ma this study, 115 ± 5 Ma by J. Gillespie) and are largely in agreement with the results obtained in Ghent as well. The larger amount of (natural) dispersion for the Adelaide results is purely due to comparing multi-grain with single-grain-results.

Apatite Fission Track Thermochronology

Radial plots for all samples are shown in Figures 5. All samples except 9582, 9508 and 7582 show a large dispersion in individual AFT ages, when dispersion was higher than ~20%, the data for these samples have been subdivided into populations of two age-components. This un-mixing process was carried out using the automatic mixture model in *Radial Plotter* and using the dispersion in D_{par} measurements (which reflects different annealing kinetics among individual grains) as a visual aid to validate the modelled age-components. Statistical acceptable minimum AFT ages and additional AHe and/or ZHe ages (discussed further) are indicated as well.

Sample 2017962 yields a central age of 273 ± 24 Ma with a large degree (36%) of dispersion. Using the automatic mixture model in *Radial Plotter* (Vermeesch 2009), two age-components were differentiated of 187 ± 11 Ma and 339 ± 14 Ma, the minimum statistical acceptable AFT age was found to be 164 ± 20 Ma. The D_{par} measurements produced an average length of 1.2 μm.

The central age for sample 2017960 is 383 ± 29 Ma with two age populations present, (1) at 475 ± 33 Ma, and (2) at 306 ± 25 Ma. The minimum age gathered from *Radial Plotter* is 293 ± 53 Ma. The individual AFT ages show minor scatter between these two age populations as well. The average D_{par} length produced was 1.27 μm with minimal dispersion.

Sample 9594 yields a central age of 403 ± 27 Ma with two main populations in the sample, (1) at 488 ± 56 Ma and (2) at 323 ± 38 Ma while the minimum age is 314 ± 42 Ma. Minor scatter of individual ages between age populations is present. The smallest D_{par} length was produced for this sample, at 0.80 μm while the average D_{par} length was 1.15 μm.

As its part of the same igneous body, 9582's AFT ages are expected to be similar to that of 9594, and the central age for sample 9582 (402 ± 46 Ma) is within error to that of 9594, however, this central age is unreliable as the sample shows rather large dispersion (29%). It was opted to exclude two significantly older outliers of about 700 Ma based on their low-uranium concentrations which brings the central age down to 342 ± 25 Ma with a dispersion of 4.6 %. This age is within error to the youngest age population observed in sample 9594 and thus validates this age population. The minimum age for the sample is 324 Ma which is only 10 Ma older than for sample 9594. The average D_{par} length of 1.13 μm is also close to the D_{par} length of 9594, further strengthening the connection between the two samples.

Sample 9528 yields a central age of 276 ± 26 Ma with large dispersion (25%). Two distinctive age populations can be defined of 325 ± 29 Ma and 188 ± 19 Ma which correlate well with the populations defined in the previously discussed samples (especially with sample 2017962). The minimum age of 196 ± 31 Ma for sample 9528 plots within error of that for sample 2017962. This sample yielded the second highest D_{par} average of all samples at 1.4 μm as well as the second highest dispersion of 1.10 – 2.00 μm.

The apatite grains in sample 9508 yield rather large U zonation and large inclusions which affected most of the obtained AFT data for this sample. Only five reliable age determinations could be used which returned a central age of 414 ± 33 Ma. The minimum AFT is reported as 413 ± 34 Ma while the D_{par} length average is 1.3 μm.

Samples 7582 and 7571 are from the same monzonite body, and since sample 7582 returned only 3 reliable ages, both samples were pooled in the same radial plot. Their pooled central age was calculated as 376 ± 28 Ma. Given the rather large age dispersion (24%), they were separated into two populations with ages of 441 ± 28 Ma and 271 ± 25 Ma which correlate well with other samples from the study area. The minimum AFT age for these pooled samples is 280 ± 38 Ma. The dispersion of D_{par} lengths within these samples is the largest of all samples from 0.90 – 2.10 μm while the average D_{par} length of 1.58 μm is also the highest of all samples.

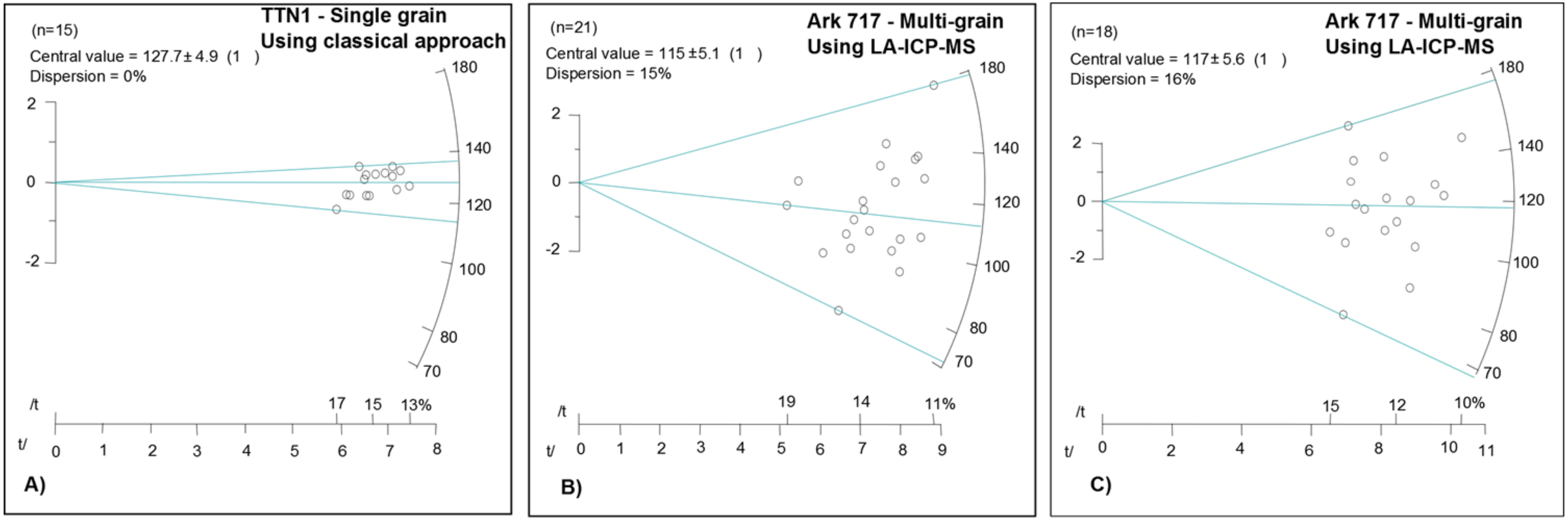

Figure 4, Radial plots of Apatite Fission Track ages from the Ark 717 Sample (b and c) and the TTN1 sample (a) detailing the ages and standard deviation of each grain counted, the average age (Central value), and the degree of dispersion. n is the number of analysed grains. a and b are radial plots from previous Apatite Fission Track studies by Dr. Stijn Glorie (a) and Mr. Jack Gillespie (b). c displays the results obtained in this study. The three samples indicate the validity of the applied method (see text for more details). Radial plots were constructed using *Radial Plotter* (Vermeesch 2009).

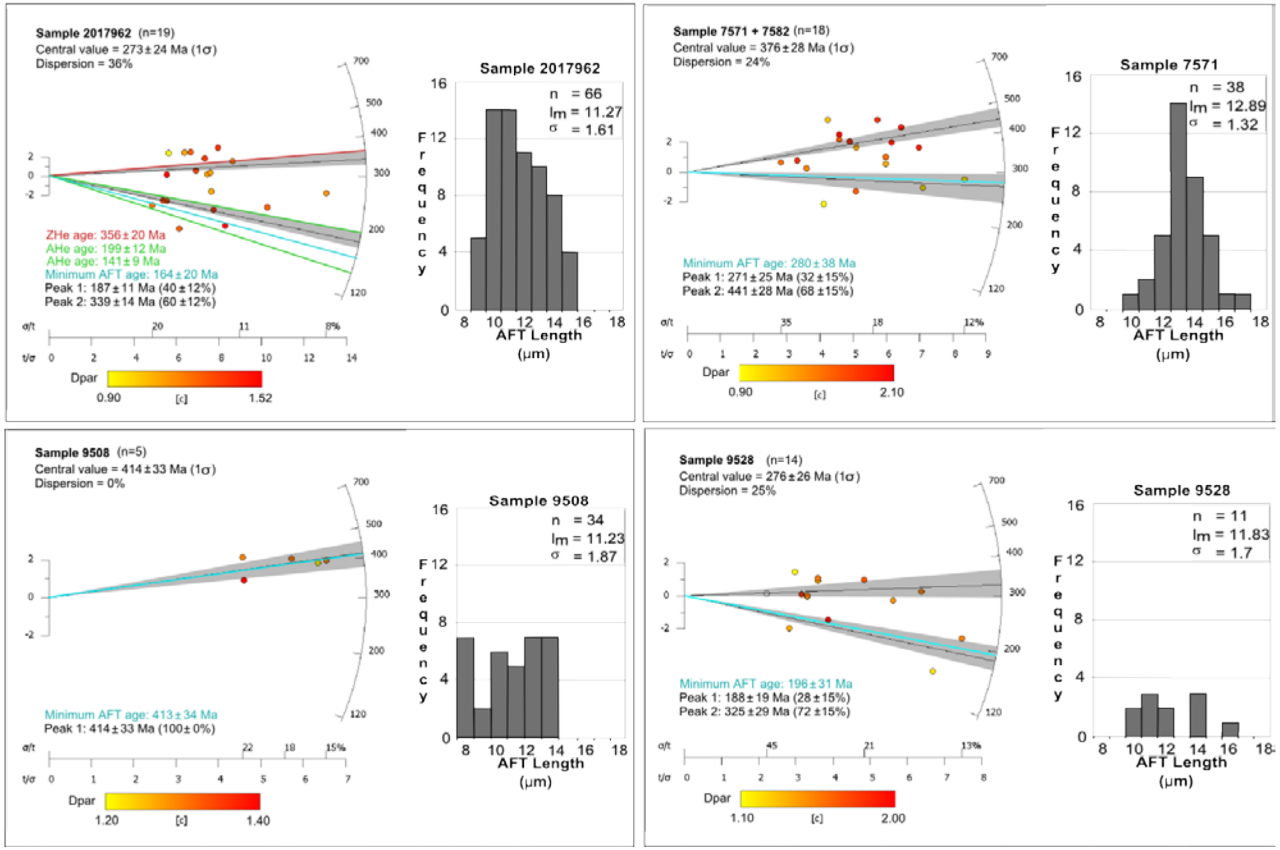

Figure 5, Radial plots of Apatite Fission Track (AFT) ages from samples 2017962, 2017960, 7571 and 9582, 9508, 9528, 9582, and 9594, as well as a radial plot containing all samples. n indicates number of grains measured, Central value indicates the central age of the sample, dispersion indicates the percentage of age dispersion within the sample, the colour difference indicates the different D_{Par} (Etch Pit) lengths for each measured grain. D_{Par} is measured in µm. Where more than one population of ages is present, the central age is split into age peaks using the Automatic Mixture model of *Radial Plotter*. All ages acquired from radial plots are presented in table 1. To the right of each radial plot is the accompanying AFT length frequency histogram for each sample (except 7582 which has no length data, only the length data for 7571 is shown). On each histogram, AFT length is in µm, n indicates the number of tracks measured, l_m is average track length, and σ is the Standard deviation of the sample. Radial plots were constructed using *Radial Plotter* (Vermeesch 2009).

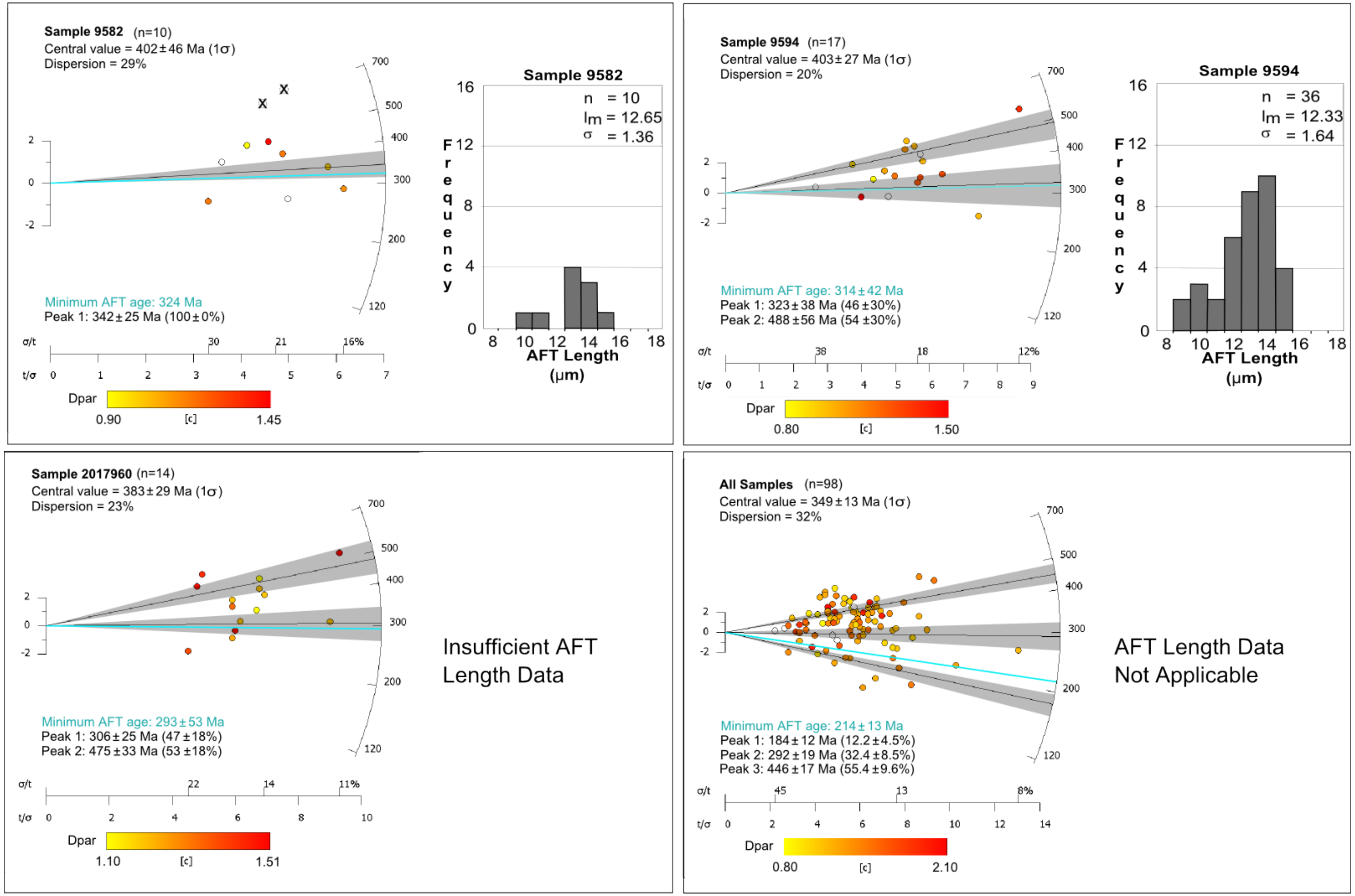

Figure 5, continued.

For one additional sample (7327) no reliable AFT age determination could be obtained due to anomalously low ^{238}U concentrations of the apatites hence no results are displayed in Figure 5 for this sample.

When all the samples are pooled on the same radial plot, three main populations can be distinguished: 446 ± 17 Ma, 292 ± 19 Ma, and 184 ± 12 Ma (Figure 5). These age populations are interpreted to represent the timing of important cooling episodes during the late Ordovician, early Permian and early Jurassic through the apatite fission track closure temperatures (~120-60 °C), recorded in the thermal history of the Peak and Denison basement. The minimum AFT age for all samples plots at 214 ± 13 Ma which is largely in agreement (slightly older) with the youngest defined age peak of 184 ± 12 Ma, indicating that the final cooling phase through AFT closure temperatures occurred at ~200Ma.

Sample	Altitude (m)	Lithology	U/Pb age	ρ_s	Ns	N	^{238}U	σ	AFT age	Lower age	Upper Age	l_m	n	σc
7571 + 7582	400	Syenite	497 ± 10	49 + 32.54	531	17	4.766 + 22.03	0.052 + 0.673	376 ± 28	271 ± 25	441 ± 28	12.89	38	1.32
9508	200	Syenite	497 ± 10	21.79	170	5	6.286	0.157	414 ± 33	-	-	11.23	34	1.87
9528	300	Monzonite	497 ± 10	13.32	293	14	9.59	0.128	276 ± 26	188 ± 19	325 ± 29	11.83	11	1.7
9582	200	Monzonite	497 ± 10	10.75	186	8	6.286	0.157	342 ± 25	-	-	12.65	10	1.36
9594	150	Monzonite	497 ± 10	10.76	538	17	5.086	0.055	403 ± 27	323 ± 38	488 ± 56	12.33	36	1.64
2017960	150	Rhyolite	1806 ± 27	11.91	611	14	7.321	0.221	383 ± 29	306 ± 25	475 ± 33	-	-	-
2017962	100	Granite	1793 ± 8	11.04	1115	19	8.786	0.128	273 ± 24	187 ± 11	339 ± 14	11.27	66	1.61

Table 1, Sample details, Apatite Fission Track (AFT) results, and U/Pb age of each sample. Measured data is also shown, where ^{238}U = concentration of ^{238}Uranium, σ = Standard Deviation of the ^{238}U, ρs = counted AFT density (in 10^5 tracks/ cm^2), Ns = number of fission tracks counted, N = number of grains counted, AFT age = Apatite Fission Track Central age (lower and upper age are all AFT age populations of their respected samples), l_m = average confined AFT length, n = number of confined tracks counted, and σc = Standard Deviation of the confined tracks.

Apatite Fission Track Length Data

AFT length histograms for all relevant samples are present in Figure 5. For samples 9528 and 9582, where less than 30 confined tracks were measured, caution was exercised towards further interpretations due to the low number of confined tracks. Sample 2017962 contained 66 measurable confined tracks, with an average length of 11.27 µm and a standard deviation of 1.61 µm. Sample 9594 yielded an average length of 12.33 µm based on 36 confined tracks with a standard deviation of 1.64 µm. Only 10 confined tracks were found for sample 9582 with an average length of 12.56 µm and a standard deviation of 1.36 µm. Much like sample 9582, sample 9528 only contained 11 measureable confined tracks. The average track length is 11.8 µm with a standard deviation of 1.7 µm. 34 confined tracks were measured in sample 9508 with an average length of 11.23 µm and a standard deviation of 1.87 µm. No AFT length data was collected for sample 7582, therefore, only AFT length data for sample 7571 is shown in Figure 5 and in Table 1. 38 confined tracks were measured with an average length of 12.89 µm and a standard deviation of 1.32 µm.

(U-Th-Sm)/He Thermochronology

Three samples were chosen to be analysed using the (U-Th-Sm)/He method at the John de Laeter Centre in Curtin University (N. Evans). Apatite grains from samples 2017962, 9582 and 7327 and zircons from 2017962 (Table 2) were chosen based on grain quality. The zircon (U-Th-Sm)/He (ZHe) results obtained for sample 2017962 show little dispersion with an average ZHe age of 356.4 ± 20.4 Ma. The apatite grains from 2017962, in comparison, produced two (U-Th-Sm)/He (AHe) age clusters of 199.6 ± 12.8 Ma based on three grains and 97.2 ± 6.6 Ma based on two grains (Table 2). The oldest AHe age component mimics the minimum AFT age for this sample. For sample

9582 an average AHe age of 101.1 ± 7.6 Ma was obtained based on 2 analyses. This AHe age corresponds well with the youngest AHe cluster for sample 2017962 and indicates that cooling through the AHe closure temperatures (~75-45 °C) occurred during the Mid Cretaceous. Furthermore, Sample 9582 yields two other AHe ages of Late Cretaceous (63.4 ± 4.7 Ma) and Miocene (16.4 ± 1.2 Ma). The latter Miocene AHe age was however only obtained for one apatite grain thus caution is required to not over-interpret this age. Sample 7327 recorded an average AHe age of 76.1 ± 6 Ma based on five grains, however, they were scattered from 88.1 Ma to 62.6 Ma which are further indications of cooling through the AHe closure temperatures during the Mid to Late Cretaceous.

Sample	*He Age*	*AFT age*	*^{238}U*	*^{232}Th*	*^{147}Sm*	*$^{232}Th/^{238}U$*	*^{4}He*	*Ft*
2017962 (ZHe)	356.4 ± 20.4	187 ± 11 339 ± 14	893.8	304.1	-	0.35	38.72	0.65
2017962 (AHe)	199.6 ± 12.8 97.2 ± 6.6	187 ± 11 339 ± 14	31.23	81.44	74.25	2.46	0.41	0.6
9582 (AHe)	101.1 ± 7.6 63.4 ± 4.7 16.4 ± 1.2	342 ± 25	44.58	65.85	20.68	3.47	0.1	0.6
7327 (AHe)	76.1 ± 6	-	10.02	42.52	26.21	4.65	0.12	0.6

Table 2, (U-Th-Sm)/He results indicating the Helium (He) age, Apatite Fission Track (AFT) Age, ^{238}Uranium concentration (parts per million), ^{232}Thorium concentration (parts per million), ^{147}Samarium concentration (parts per million), Ratio of ^{232}Thorium over ^{238}Uranium, concentration of ^{4}Helium (nanocubic centimetre (ncc) per µg), and Ft (the fraction of Alpha particle ejection dependant on the dimensions the apatite crystal; Ehlers and Farley 2003).

Modelling

The exhumation history of the region was modelled using the computer software *HeFTy* (Ketcham 2005) which models the path the rocks travelled in time-temperature space from a set time to the present using a combination of AFT age and length data, He age data, U and other geological significant constraints. In order to create a statistically acceptable model, fission tracks age and length data is the minimum input requirement and length data should at least include >20 confined track measurements. This condition was only met for samples 2017962, 9594, 9508 and 7571. These samples were modelled using their AFT age (and if possible AHe/ZHe) constraints, a high and low temperature endpoint at pre-Delamerian times and present-day outcrop temperatures and one additional geological constraint: all samples were assumed to be at or near the surface during the late Permian due to the presence of the Mount Margaret Surface (MMS; Rogers and Freeman 1994).

Most models produced similar results with a general trend of fast exhumation from 500 Ma to 400- 300 Ma, where the samples reach the surface, followed by shallow burial and subsequent shallow exhumation during the Cretaceous. The applied modelling software is mainly designed to model low-temperature cooling (below ~200C), the extent and timing of the thermal history above these temperatures cannot precisely be estimated using these models. As mentioned above, it is assumed that all samples started were at significant depth (and high temperatures) prior to the Delamerian.

The samples for which little thermochronological data was available (only AFT results; 9594, 9508 and 7571) show a general exhumation history of rapid exhumation from Delamerian times to ~400 Ma followed by slow cooling or thermal quiescence between ~350 and 250 Ma. All models except 9508 show shallow (to about 50 – 75 ° C) burial during the Jurassic and exhumation to the surface during the Cretaceous (Figure 6). 9508, on the other hand, shows shallow burial from ~250 Ma to ~75 Ma before rapid Cretaceous exhumation reinstated the rocks at the surface. All these samples were modelled with a goodness of fit merit for good paths (pink paths in Figure 6) of 0.5 (Table 3) and a goodness of fit merit for acceptable paths (green paths in Figure 6) at 0.05.

2017962 is the best constrained model, which is based on a combination of ZHe, AHe, AFT and geological data, therefore it produces the most plausible cooling model. However, due to the larger number of inserted data, the merit value to obtain statistically good model paths was brought down to 0.2 instead of 0.5. The Wurriecurrie Granite formed during the Mesoproterozoic, however first signs of cooling below ~200 °C were dated to the Carboniferous. Previous exhumation pulses that induced cooling below ~200 °C before the Carboniferous may have existed but are erased by the subsequent thermal history of the Ranges. This model shows that gentle early Palaeozoic cooling brought the samples to temperatures of ~200 °C before increased cooling during the Devonian – Carboniferous brought the basement to the surface. Geological evidence for early Permian surfacing comes from the occurrence of the MMS. Subsequent burial (to 75 – 80 °C) occurred from about 300 Ma to about 150 Ma before another pulse of rapid cooling carried the sample up to the near surface. A final phase of burial occurred from 150 Ma to 100 Ma before a final pulse of Cretaceous cooling brought the sample to the surface during the Late Cretaceous.

Sample	Paths tried	Acceptable paths	Good paths	Acceptable merit	Good merit
2017962	278491	2848	10	0.05	0.2
9594	10000	637	271	0.05	0.5
9508	35498	808	19	0.05	0.5
7571	10000	440	133	0.05	0.5

Table 3, *HeFTy* parameters including number of paths tried, number of acceptable paths, number of good paths, goodness of fit for acceptable paths merit, and goodness of fit for good paths merit for the four samples (2017962, 9594, 9508, and 7571).

Figure 6 (next page), the exhumation histories of samples 2017962, 7571, 9508 and 9594, modelled with the *HeFTy* software (Ketcham 2005). Each time – temperature plot illustrates the modelled pathway for each sample from 400 °C at 500 – 600 Ma to surface temperatures at the present. Each sample is constrained by measured constraints (such as Apatite Fission Track (AFT) ages, Apatite Helium (AHe) ages, or Zircon Helium (ZHe) ages; indicated by red boxes on each plot) from this thesis, geological constraints (Indicated by blue boxes on each plot) such as the Mount Margaret Surface, and a high temperature starting constraint (indicated by a black box on each plot), where the rocks are assumed to be from 450 – 600 Ma. The dashed red box on sample 2017962 indicates a constraint based on AHe data, which needed a slight shift towards lower temperatures to find a sufficient number of statistically good model paths. The green region on each plot is the acceptable path envelope, while the pink region is the good path envelope. The merits for these paths are stated in table 3.

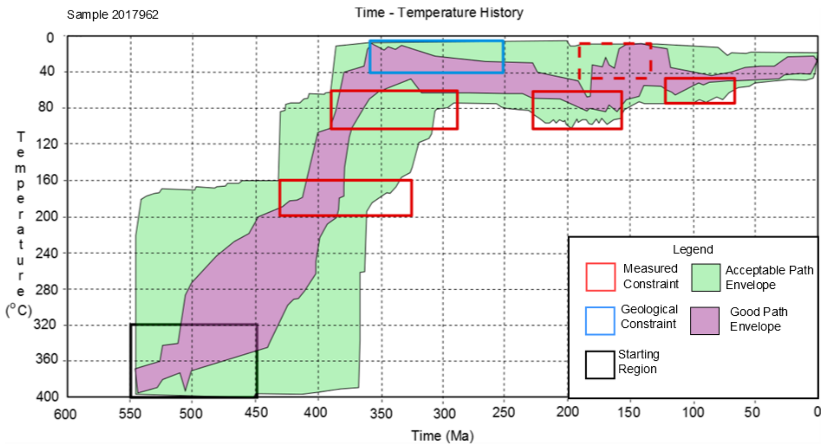
Sample 2017962
Time - Temperature History
Temperature (°C)
Time (Ma)
Legend
Measured Constraint
Acceptable Path Envelope
Geological Constraint
Good Path Envelope
Starting Region

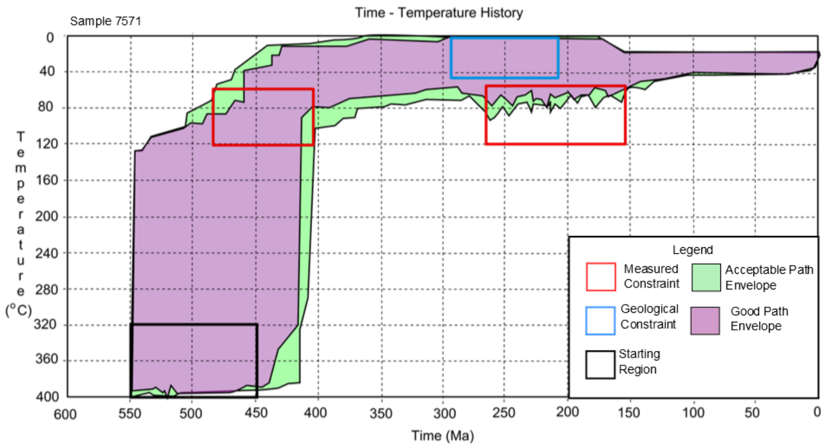
Sample 7571
Time - Temperature History
Temperature (°C)
Time (Ma)
Legend
Measured Constraint
Acceptable Path Envelope
Geological Constraint
Good Path Envelope
Starting Region

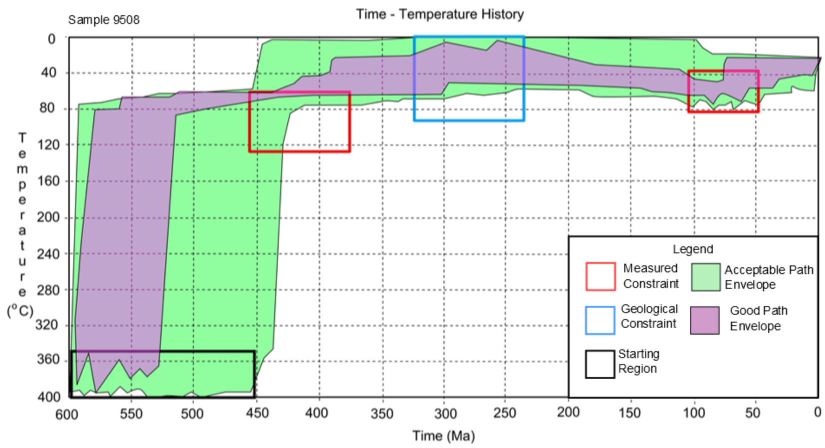
Sample 9508
Time - Temperature History
Temperature (°C)
Time (Ma)
Legend
Measured Constraint
Acceptable Path Envelope
Geological Constraint
Good Path Envelope
Starting Region

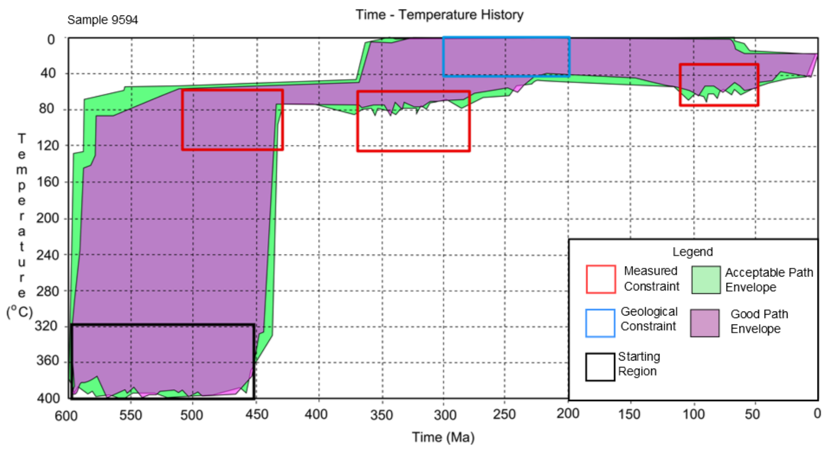
Sample 9594
Time - Temperature History
Temperature (°C)
Time (Ma)
Legend
Measured Constraint
Acceptable Path Envelope
Geological Constraint
Good Path Envelope
Starting Region

DISCUSSION

All the *HeFTy* models produced in this thesis are indicative of fast cooling from the Delamerian to 400 – 350 Ma before reaching the surface at 300 – 250 Ma, although these models are highly plausible, they do not account for the ZHe age at ca. 356 Ma. This ZHe age would mean the rocks underwent burial from AFT temperatures to ZHe temperatures from 400 Ma to 356 Ma before returning to AFT closure temperatures, which is not witnessed in any *HeFTy* model. After 250 Ma, and depending on the sample, these models either indicate that (1) the rocks stayed at or near the surface from 250 Ma to the present or (2) minor burial occurred from 250 Ma to about 150 Ma, followed by rapid shallow exhumation to the surface where the rocks remained to the present. As illustrated above, none of the *HeFTy* models are unambiguous and fully encompass the full exhumation history of the Ranges as no model takes all obtained thermochronological data into account. For this reason, a model which fits all data (including geological constraints) was created (Figure 7).

Figure 7 a shows the preferred thermal history model based on all obtained data for this thesis and matched with the sedimentological record of the Peake and Denison Ranges. This section first discusses the data obtained by the different thermochronometers for this thesis, before commenting on the model itself and the tectonic events which controlled the exhumation. This is followed by, comparisons and interpretations between neighbouring regions and the Peake and Denison Ranges. Finally, the previous the validity of the previous models are discussed.

Thermochronological constraints

The results of the AFT analysis on all samples indicate three major periods of rapid cooling which are interpreted as episodes of significant exhumation in the Peake and

Denison Ranges. Ordovician (~470-440 Ma) and Carboniferous – early Permian (~340-290 Ma) exhumation pulses can be related with the well-known, regional Delamerian and Alice Springs Orogenies while the younger Jurassic (~200-180 Ma) event can be related to a local exhumation event or linked to possible increased hydrothermal activity in the region at that time (as discussed below).

The Late Devonian ZHe ages obtained in this thesis are only a few Ma older than the Carboniferous AFT ages and record evidence for rapid exhumation at that time.

The AHe ages for this study indicate cooling within the last 200 Ma with a main cooling phase during the Mid to Late Cretaceous, however, due to the evidence for the Ranges reaching the surface during the Permian as seen by the presence of the Mount Margaret Surface and the older AFT ages, it is unlikely these indicate any deep exhumation.

Three AHe ages fall outside of the Mid to Late Cretaceous, being ~199 Ma, 141 Ma, and 16 Ma. The oldest AHe age may indicate (1) the early stages of burial to AFT temperatures or the presence of hydrothermal activity during that time as mentioned above. This AHe age is slightly older than the youngest AFT ages within the region which points towards an increase in temperature from ~200 Ma to ~180 Ma and therefore, most likely an increase in burial rates in the region. The alternative has already been noted in this thesis with the possibility of hydrothermal activity during this time causing the increased temperatures as it correlates with a period of hydrothermal activity within the Arkaroola region (Weisheit *et al*. 2014).

The single AHe age at ca. 141 Ma is an indicator of minor burial at that time, which is supported by the deposition of Algebuckina Sandstone and the Neales River Group sediments (both shown in blue on the sedimentary log on Figure 7).

The youngest AHe age is likely related to the Miocene fault movement which was observed by Wopfner (1968). Since there is only one grain producing this age, it is unlikely to be a major exhumation event. However, it is possible that this AHe age can be linked with the final exhumation event in the Ranges with burial from 50 Ma to around 20 Ma before the rocks were rapidly exhumed to the surface through fault movement.

Thermal history model for the Peake and Denison Ranges

The thermal history model presented in Figure 7 a was fitted through all the data points whilst matching it with the sedimentary data presented by Rogers and Freeman (1994). The most likely model shows fast cooling and exhumation during the Delamerian Orogeny (~500 Ma). However, these Delamerian AFT ages were unsupported by ZHe data collected from sample 2017962. This may point towards two possible exhumation paths in the model (dashed lines versus filled lines). The first model indicates that the Ranges exhumed rapidly from 500 Ma to 400 Ma and was followed by erosion and sedimentation (as seen in the poorly constrained Nultaddy Seismic Unit which deposited during this time), which caused burial of the Ranges until reaching temperatures around 200 °C at ~350 Ma. At this point, another pulse of the Alice Springs Orogeny would have forced the Ranges out of ZHe closure temperatures and into AFT closure temperatures within a few million years.

The alternative model (dashed lines) shows that the Wirricurrie granite (sample 2017962) experienced a different thermal history compared to the western Peake and Denison Ranges as this granite is located on the opposite side of a major fault (Figure 2). In this model, the ZHe age of 356 Ma may be the first time the Wirriecurrie Granite cooled to low temperatures while the western Ranges where exhumed to similar temperatures at an earlier time (~490 Ma). This model would rely on the existence of the fault in the Denison Range during this time and its movement facilitating the uplift of the Wirriecurrie Granite while the rest of the Ranges experienced less uplift. Since neither path can be proven, both have been indicated on Figure 7.

After the Ranges abandoned ZHe temperatures, rapid exhumation occurred which was quickly followed by with the deposition of, the Boorthanna, Stuart Range, and Mount Toondina Formations at ~300 Ma. Since the model does not display evidence of burial during this time, the rocks remained likely at the subsurface. After this time, the presence of the Mount Margaret Surface provides evidence for the region reaching the surface at 250 Ma, which is clearly displayed in the model. At ~200Ma AFT and AHe data indicate either burial or the previously mentioned hydrothermal activity. Neither path can be ruled out due to lack of evidence for both theories.

From 150 Ma to 100 Ma, a period of shallow burial and deposition occurred, as reflected in the deposition of the Algebuckina Sandstone and the Neales River Group sediments. The Late Cretaceous is characterised by a hiatus in the sedimentary record which correlates remarkably well with the ~100-60 Ma AHe ages obtained for this study. Both observations are indicative of a period of renewed exhumation after sedimentary burial brought the basement rocks down to ~80 °C. It is assumed that, by the end of this exhumation, the Peake and Denison Ranges are fully exposed at the surface. Immediately following the end of the Cretaceous, sedimentation resumed with the deposition of the Mirackina Conglomerate as well as numerous unnamed formations and sediments throughout the Cenozoic. The Miocene AHe age coincides well with increased coarse sedimentation which is likely related with fault movements as discussed above (Wopfner 1968). It is hence likely that the fault movements induced a different Cenozoic exhumation model for the eastern section of the Ranges as shown by the Cenozoic dashed path in Figure 7. While the western Ranges likely surfaced during the Late Cretaceous, the eastern section may have remained buried until the Miocene fault movement induced the present-day relief, exposing the eastern section at that time.

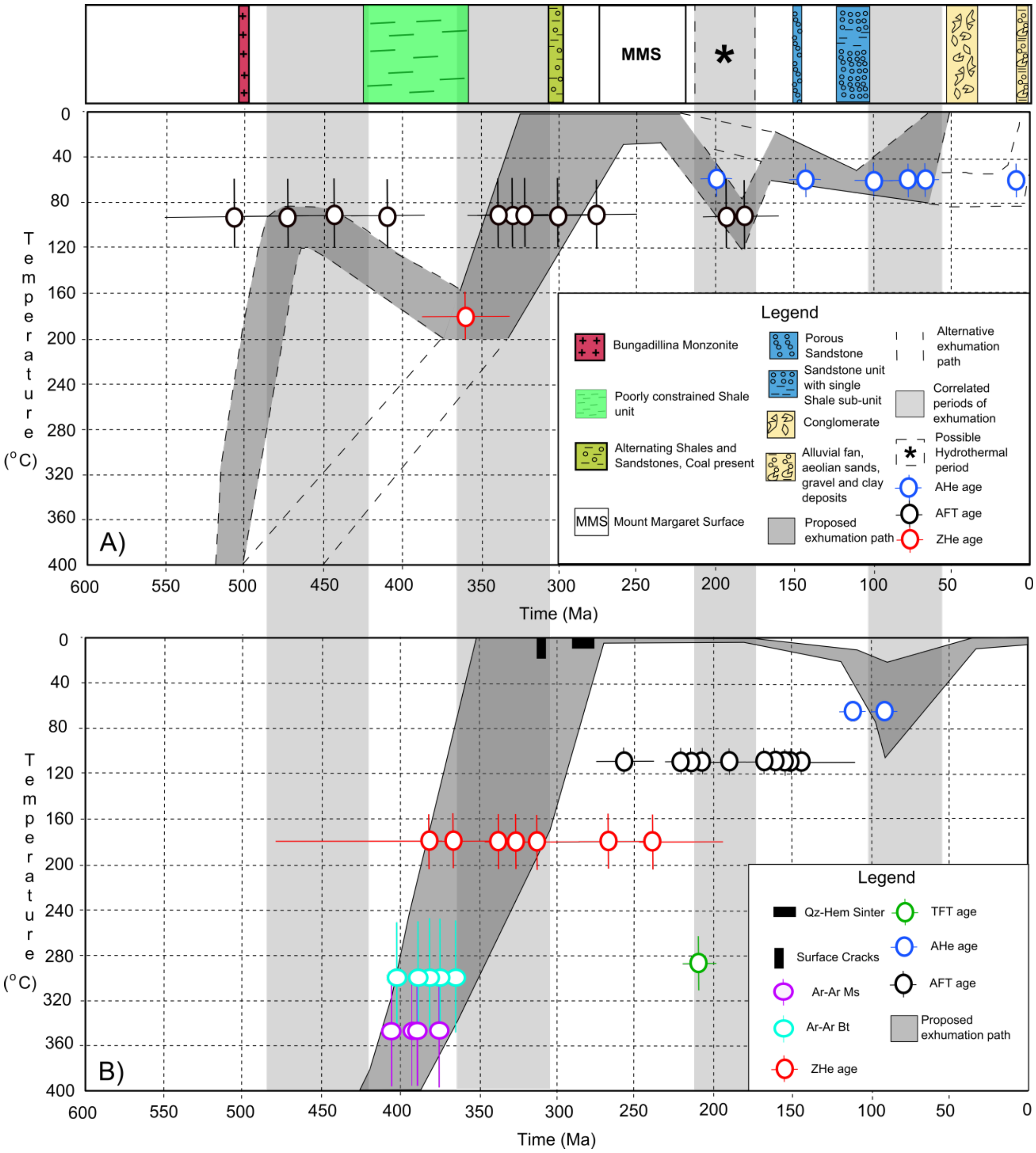

Figure 7, the proposed exhumation path of the Peake and Denison Ranges through time-temperature space (Panel a) with inclusion of sedimentary constraints and compared to the exhumation history model of the Arkaroola region (Panel b; Weisheit *et al.* 2014). Apatite Helium (AHe) ages are indicate by blue dots, Zircon Helium (ZHe) ages by red dots, and Apatite Fission Track age populations by black dots. Through these ages, a best-fit exhumation model was constructed which matches all data, the sedimentological record of the adjacent basins and the estimated cooling rates from the *HeFTy* models. Alternative exhumation paths are indicated by dashed lines (see text for discussion). The erosional peneplain which is known as the Mount Margaret Surface is also plotted since this is a period of time where the rocks are known to be at the surface. the box containing the asterisk is a period of known hydrothermal activity in the Arkaroola region and possible hydrothermal activity in the Peake and Denison Ranges. The Arkaroola region time-temperature graph was adapted from Weisheit *et al.* (2014) and contains compiled data from e.g. Krieg *et al.* (1995); McLaren *et al.* (2002); Mitchell *et al.* (2002).

Tectonic events that affected the Peake and Denison Ranges

The oldest exhumation pulse is a result of the Delamerian Orogeny (514 - 490 Ma; Foden *et al*. 2006) as it perfectly coincides with the oldest AFT ages that was interpreted to be the mechanism for the formation of the Bungadillina Monzonite (Ambrose *et al*. 1981; Morrison 1989; Rogers and Freeman 1994), However, an early pulse of the Alice Springs Orogeny (475 ± 4 Ma) may have contributed as well (Hand *et al*. 1999; Mawby *et al*. 1999; Haines *et al*. 2001). The Alice Springs Orogeny has been widely documented (e.g. Mitchell *et al*. 1998; Gibson and Stüwe 2000; Mitchell *et al*. 2002) to have caused exhumation in South Australia as it caused substantial crustal thickening throughout South Australia (Ballèvre *et al*. 2000). It is therefore likely that both orogenies had an effect on the Peake and Denison Ranges and the Ordovician exhumation pulse is thus presumably an effect of both. Unlike the previously mentioned exhumation events, the Triassic - Jurassic event is not widespread as it is not seen in distal studies (O'Sullivan *et al*. 1995; Gleadow *et al*. 2002b; Kohn *et al*. 2002), however, it has effected proximal regions such as the Cooper Basin (Mavromatidis 2007). Therefore, this period of exhumation is either a result of local exhumation or the AFT ages were partially reset by hydrothermal activity. This hydrothermal activity was observed in the Arkaroola Region as well (Figure 7; Lambert *et al*. 1982; Idnurm and Heinrich 1993; Weisheit *et al*. 2014). This hydrothermal activity has been observed by many (Ambrose *et al*. 1981; Morrison 1989; Hopper 2001), however an age for it has never been given. Alternatively, the Jurassic cooling pulse captured in the AFT data could reflect a period of shallow exhumation which is however unsupported by the occurrence of sediments of this age. Alternatively, these sediments may have been reworked and redeposited during subsequent exhumation pulses. In the latter case, these 200 - 180 Ma AFT ages may not be a result of hydrothermal activity and might just be evidence of burial and subsequent uplift of the Ranges. The final exhumation event occurred during the Cretaceous and despite the lack of explanations for the regional Cretaceous exhumation for South Australia (Gibson and Stüwe 2000; MacDonald *et al*. 2013), it is probable this exhumation was the result of the rifting of Australia from Antarctica as Stump and Fitzgerald (1992) linked exhumation during this time period in Antarctica to the rifting.

Comparison with exhumation studies on neighbouring regions

When compared to other regions in South Australia, the Peake and Denison Ranges reveal quite a few similarities with many other exhumation models. As seen in Figure 7 b, Arkaroola is one region which contains a comparable exhumation history. As shown, the Weisheit *et al*. (2014) model reveals similar AFT, ZHe and AHe results for the Arkaroola region with AFT peaks around 200 – 180 Ma, their model first reached the surface at a similar time, and both show burial before Cretaceous exhumation occurred. Three out of the four periods of exhumation highlighted in the Peake and Denison Ranges are also present in the Arkaroola Region, while no evidence for pre-Devonian upper crustal exhumation was obtained for the Arkaroola region. This may have been erased by subsequent events as the total amount of exhumation in the Arkaroola region during the Devonian-Carboniferous is estimated to be over 10km (Weisheit *et al*. 2014). The models mainly differ around 200 Ma, where the Peake and Denison model follows the data with an apparent reheating episode at ~200 Ma as a result of either deep burial or hydrothermal activity and prolonged burial during the Mid to Late Cretaceous. The Arkaroola model on the other hand explains the data solely by the hydrothermal activity during that time and maintains its position at the surface.

Another model for Arkaroola, presented by Mitchell *et al*. (2002), proposed that Arkaroola remained within the Partial Annealing Zone from the Alice Springs Orogeny until ~50 Ma, at which point it exhumed to the surface. This model matches to a certain degree, with the Peake and Denison model, however, the exhumation occurred slightly later than proposed in the Peake and Denison model for this thesis. The Mitchell *et al*. (2002) models show a clustering of AFT ages around 200 Ma which correlates to the youngest AFT cluster in the Peake and Denison Ranges, and with the model by Weisheit *et al*. (2014) for Arkaroola. The Mitchell *et al*. (2002) model furthermore suggests that exhumation occurred during the Late Cretaceous, similar as shown for the Peake and Denison Ranges in this thesis.

This Late Cretaceous exhumation is also present within the Adelaide Fold Belt of South Australia (Gibson and Stüwe 2000). A Carboniferous – Permian exhumation even is recorded for this region which correlates well with the contemporaneous AFT population within the Peake and Denison Ranges. More regional studies (Gleadow *et al*. 2002b; Kohn *et al*. 2002) of South Australia postulate that Carboniferous exhumation occurred throughout most of South Australia while Boone (2013) provides further thermochronological evidence for exhumation during the Devonian – Carboniferous. These matching models from various locations within South Australia indicate that the Peake and Denison Ranges have a similar exhumation history with the other study regions in South Australia at least during the Palaeozoic. The Meso-Cenozoic thermal history of the Peake and Denison Ranges slightly differs of that of other study regions (as discussed above), which may partly be related with the absence of AHe or other low-temperature data in other studies.

Regional interpretations and models

Before this research was conducted, three theories existed on the exhumation of the Peake and Denison Ranges. Radke (1973), proposed a tectonic event at 266 Ma from AFT data which is only marginally younger than obtained for some samples in this thesis (e.g. the 273 Ma population of sample 2017962). The presence of the Mount Margaret Surface around this time proves there was exhumation during this time. This is also the first time the Ranges are known to be at the surface which validates Radke's proposition of a tectonic event during this time. The single AHe age in the Miocene gives weight to Wopfner's argument to fault movement during this time, however, it is likely to be only minor in terms of exhumation of the Ranges. The third theory, from MacDonald *et al*. (2013) postulated that widespread exhumation occurred in the northern Gawler Craton during the Cretaceous which was observed for the model for the Peake and Denison Ranges and within the Arkaroola model as well. MacDonald also proposed the Ceduna Delta (Figure 1) formed from a proximal and distal source, over two different time periods during the Cretaceous (Santonian – Maastrichtian and Cenomanian). The results obtained for this thesis provide evidence for exhumation during the Cenomanian (~100-95Ma AHe ages) and Maastrichtian (~75-60 Ma AHe ages). However none of these events are well-constrained in the thermal history model of the Peake and Denison Ranges and may rather indicate that continuous exhumation occurred during the late Cretaceous until the end of the Maastrichtian. Although more data is required to verify the extent of the Late Cretaceous exhumation, our data indicates that significant topography existed in the Peake and Denison Ranges since the early Cenomanian. This topography would have acted as a barrier for a major river system that is thought to have existed at that time (Figure 1; McDonald *et al*. 2013). However, the exhumation events recorded in the Peake and Denison Ranges during the

Cenomanian and Maastrichtian may have induced transport of sediments from South Australia`s interior towards the Bight basin. In this regard, previously deposited outwash of river systems within Central Australia may have been reworked and transported southwards as a result of these Late Cretaceous exhumation pulses.

CONCLUSIONS

Low-temperature thermochronology of the Peake and Denison Ranges revealed two major periods of exhumation, during the Ordovician and late Carboniferous – Permian, and two periods of shallow exhumation, after sedimentary burial or hydrothermal activity, during the Late Triassic – Jurassic and the Cretaceous.

The combination of the Delamerian and Alice Springs Orogenies induced exhumation of the Peake and Denison Ranges to shallow crustal levels. As a result, the basement cooled to surface temperatures from temperatures in excess of 400 °C, over two bursts of exhumation at ~500 – 430 Ma and 350 – 300 Ma. Latter phase exhumed the Peake and Denison Ranges to the surface which is recorded by the presence of the Mount Margaret Surface around 250 Ma. Subsequent burial or hydrothermal activity brought the Ranges back into AFT and AHe temperatures at around 200 – 180 Ma. From 140 – 100 Ma, the Ranges were occupying AHe temperatures due to shallow burial and deposition of the Aglebuckina Sandstone and Neales River Group sediments. Immediately after deposition ceased, the final exhumation period began with the long, shallow Cretaceous exhumation from AHe temperatures to the surface which was potentially caused by the rifting of Australia from Antarctica.

The proposed exhumation model for this thesis confirms the prior theories of Permian tectonism, widespread Cretaceous exhumation and Miocene fault movement, plus additional events which transported the Peake and Denison Ranges to the surface.

The Peake and Denison Ranges experienced a similar exhumation history as the northern Flinders Ranges, as seen in Figure 7. Studies of the Adelaide Fold Belt indicate there are at least two shared exhumation events with the Peake and Denison Ranges, one in the Carboniferous–Permian and the other in the Cretaceous, while other regional South Australia studies share an obvious exhumation pulse during the Carboniferous.

ACKNOWLEDGMENTS

This thesis was made possible thanks to the financial support of Department of State Development, South Australia and the University of Adelaide. I would like to thank Stijn Glorie for the countless hours of supervision, Dr. Anthony Reid and Prof. John Foden for the sample donations, Prof. Alan Collins for his supervision, Jack Gillispie, Max Reddy, Rachel Rudd and Natalie Debenham for numerous discussions about the thesis, The John De Laeter Center at Curtin University for collecting the He data, and lastly, Adelaide Microscopy for the use of the LA-ICP-MS.

REFERENCES

ALLENDER J. F., TAYLOR B. W. & GILBY A. R. 1987. Geophysical interpretations report. 1984 Hogarth-ARC. PELs 5 and 6 Arckaringa Block. *South Australia Department of Mines and Energy. Open File Envelope* 5561(6). (unpublished).

AMBROSE G. J., FLINT R. B. & WEBB A. W. 1981. Precambrian and Palaeozoic Geology of the Peake and Denison Ranges. *Geological Survey of South Australia Bullitin* **50**.

BAKKER R., J. & ELBURG M. 2006. A magmatic- hydrothermal transition in Arkaroola (Northern Flinders Ranges, South Australia): from diopside-titanite pegmatites to hematite-quartz growth. *Contributions to Mineralogy and Petrology* **152**, 541-569.

BALLÈVRE M., MÖLLER A. & HENSEN B. J. 2000. Exhumation of the lower crust during crustal shortening: an Alice Springs (380 Ma) age for a prograde amphibolite facies shear zone in the Strangways Metamorphic Complex (central Australia). *Journal of Metamorphic Geology* **18**, 737-747.

BOONE S. C. 2013. Apatite Fission Track Anomaly within the Archean-Proterozoic Gawler Craton: The Thermal Record of a Paleoaquifer System. Masters Thesis. University of Melbourne, Melbourne (unpubl.).

BRUGGER J., FODEN J. & WULSER P.-A. 2011. Genesis and preservation of a uranium-rich paleozoic epithermal system with a surface expression (Northern Flinders Ranges, South Australia): radiogenic heat driving regional hydrothermal circulation over geological timescales. *Astrobiology* **11**, p.499+.

DE GRAVE J., GLORIE S., RYABININ A., ZHIMULEV F., BUSLOV M. M., IZMER A., ELBURG M., VANHAECKE F. & VAN DEN HAUTE P. 2012. Late Palaeozoic and Meso-Cenozoic tectonic evolution of the southern Kyrgyz Tien Shan: Constraints from multi-method thermochronology in the Trans-Alai, Turkestan-Alai segment and the southeastern Ferghana Basin. *Journal of Asian Earth Sciences* **44**, 149-168.

EHLERS T. A. & FARLEY K. A. 2003. Apatite (U–Th)/He thermochronometry: methods and applications to problems in tectonic and surface processes. *Earth and Planetary Science Letters* **206**, 1-14.

ELBURG M. A., BONS P. D., FODEN J. & BRUGGER J. 2003. A newly defined Late Ordovician magmatic–thermal event in the Mt Painter Province, northern Flinders Ranges, South Australia. *Australian Journal of Earth Sciences* **50**, 611-631.

ELBURG M. A., ANDERSEN T., BONS P. D., SIMONSEN S. L. & WEISHEIT A. 2013. New constraints on Phanerozoic magmatic and hydrothermal events in the Mt Painter Province, South Australia. *Gondwana Research* **24**, 700-712.

FANNING C. M., FLINT R. B., PARKER A. J., LUDWIG K. R. & BLISSETT A. H. 1988. Refined Proterozoic evolution of the Gawler Craton, South Australia, through U-Pb zircon geochronology. *Precambrian Research* **40–41**, 363-386.

FANNING C. M., REID A. J. & TEALE G. 2007. A geochronological framework for the Gawler Craton, South Australia. . *South Australia. Geological Survey. Bulletin* **55**.

FARLEY K. A. 2002. (U-Th)/He Dating: Techniques, Calibrations, and Applications. *Reviews in Mineralogy and Geochemistry* **47**, 819-844.

FODEN J., ELBURG M. A., DOUGHERTY-PAGE J. & BURTT A. 2006. The Timing and Duration of the Delamerian Orogeny: Correlation with the Ross Orogen and Implications for Gondwana Assembly. *The Journal of Geology* **114**, 189-210.

FOSTER D. A., MURPHY J. M. & GLEADOW A. J. W. 1994. Middle tertiary hydrothermal activity and uplift of the northern flinders ranges, South Australia: Insights from apatite fission-track thermochronology. *Australian Journal of Earth Sciences* **41**, 11-17.

GIBSON H. J. & STÜWE K. 2000. Multiphase cooling and exhumation of the southern Adelaide Fold Belt: constraints from apatite fission track data. *Basin Research* **12**, 31-45.

GLEADOW A. J. W., DUDDY I. R., GREEN P. F. & HEGARTY K. A. 1986. Fission track lengths in the apatite annealing zone and the interpretation of mixed ages. *Earth and Planetary Science Letters* **78**, 245-254.

GLEADOW A. J. W., BELTON D. X., KOHN B. P. & BROWN R. W. 2002a. Fission Track Dating of Phosphate Minerals and the Thermochronology of Apatite. *Reviews in Mineralogy and Geochemistry* **48**, 579-630.

GLEADOW A. J. W., KOHN B. P., BROWN R. W., O'SULLIVAN P. B. & RAZA A. 2002b. Fission track thermotectonic imaging of the Australian continent. *Tectonophysics* **349**, 5-21.

GREEN P. F., DUDDY I. R., GLEADOW A. J. W., TINGATE P. R. & LASLETT G. M. 1985. Fission-track annealing in apatite: Track length measurements and the form of the Arrhenius plot. *Nuclear Tracks and Radiation Measurements (1982)* **10**, 323-328.

HAINES P. W., HAND M. & SANDIFORD M. 2001. Palaeozoic synorogenic sedimentation in central and northern Australia: a review of distribution and timing with implications for the evolution of intracontinental orogens. *Australian Journal of Earth Sciences* **48**, 911-928.

HAND M., MAWBY J. O., KINNY P. & FODEN J. 1999. U–Pb ages from the Harts Range, central Australia: evidence for early Ordovician extension and constraints on Carboniferous metamorphism. *Journal of the Geological Society* **156**, 715-730.

HASEBE N., BARBARAND J., JARVIS K., CARTER A. & HURFORD A. J. 2004. Apatite fission-track chronometry using laser ablation ICP-MS. *Chemical Geology* **207**, 135-145.

HOPPER D. J. 2001. Crustal evolution of paleo- to mesoproterozoic rocks in the Peake and Denison Ranges, South Australia. PhD Thesis. The University of Queensland, Brisbane (unpubl.).

IDNURM M. & HEINRICH C. A. 1993. A palaeomagnetic study of hydrothermal activity and uranium mineralization at Mt Painter, South Australia. *Australian Journal of Earth Sciences* **40**, 87-101.

KETCHAM R. A. 2005. Forward and Inverse Modeling of Low-Temperature Thermochronometry Data. *Reviews in Mineralogy and Geochemistry* **58**, 275-314.

KOHN B. P., GLEADOW A. J. W., BROWN R. W., GALLAGHER K., O'SULLIVAN P. B. & FOSTER D. A. 2002. Shaping the Australian crust over the last 300 million years: insights from fission track thermotectonic imaging and denudation studies of key terranes. *Australian Journal of Earth Sciences* **49**, 697-717.

KRIEG G. W., ALEXANDER E. M. & ROGERS P. 1995 Eromanga Basin. In DREXEL J. F. & PREISS W. V. eds. The Geology of South Australia, vol. 2, The Phanerozoic. South Australia Geological Survey, Bulletin. pp. 101-105.

LAMBERT I. B., DREXEL J. F., DONNELLY T. H. & KNUTSON J. 1982. Origin of breccias in the Mount Painter area, South Australia. *Journal of the Geological Society of Australia* **29**, 115-125.

LI G.-M., CAO M.-J., QIN K.-Z., EVANS N. J., MCINNES B. I. A. & LIU Y.-S. 2014. Thermal-tectonic history of the Baogutu porphyry Cu deposit, West Junggar as constrained from zircon U–Pb, biotite Ar/Ar and zircon/apatite (U–Th)/He dating. *Journal of Asian Earth Sciences* **79, Part B**, 741-758.

MACDONALD J., D., HOLFORD S. P., GREEN P. F., DUDDY I. R., KING R. C. & BACKÉ G. 2013. Detrital zircon data reveal the origin of Australia's largest delta system. *Journal of the Geological Society, London* **170**, 3-6.

MAVROMATIDIS A. 2007. Exhumation Study in the Cooper-Eromanga Basins, Australia and the Implications for Hydrocarbon Exploration. *Energy Sources, Part A: Recovery, Utilization, and Environmental Effects* **29**, 631-648.

MAWBY, HAND & FODEN 1999. Sm–Nd evidence for high-grade Ordovician metamorphism in the Arunta Block, central Australia. *Journal of Metamorphic Geology* **17**, 653-668.

MCDOWELL F. W., MCINTOSH W. C. & FARLEY K. A. 2005. A precise 40Ar–39Ar reference age for the Durango apatite (U–Th)/He and fission-track dating standard. *Chemical Geology* **214**, 249-263.

MCLAREN S., DUNLAP W. J., SANDIFORD M. & MCDOUGALL I. 2002. Thermochronology of high heat-producing crust at Mount Painter, South Australia: Implications for tectonic reactivation of continental interiors. *Tectonics* **21**, 2-1-2-18.

MCLAREN S., SANDIFORD M., POWELL R., NEUMANN N. & WOODHEAD J. 2006. Palaeozoic Intraplate Crustal Anatexis in the Mount Painter Province, South Australia: Timing, Thermal Budgets and the Role of Crustal Heat Production. *Journal of Petrology* **47**, 2281-2302.

MITCHELL M. M., KOHN B. P. & FOSTER D. A. 1998 Phanerozoic cooling in eastern South Australia: consequences for tectonic models. In P. V. D. H. & F. D. C. eds. Advances in Fission-Track Geochronology: a Selection of Papers Presented at the International Workshop on Fission Track Dating. pp. 207-224. Ghent, Belgium: Kluwer Academic Publishers. 1996.

MITCHELL M. M., KOHN B. P., O'SULLIVAN P. B., HARTLEY M. J. & FOSTER D. A. 2002. Low-temperature thermochronology of the Mt Painter Province, South Australia. *Australian Journal of Earth Sciences* **49**, 551-563.

MORRISON R. S. 1989. The Igneous Intrusive Rocks of the Peake and Denison Ranges within the Adelaide Geosyncline Volume II: Figures, Plates, Captions, Maps, Tables and Appendicies. PhD Thesis. University of Adelaide, Adelaide (unpubl.).

O'SULLIVAN P. B., KOHN B. P., FOSTER D. A. & GLEADOW A. J. W. 1995. Fission track data from the Bathurst Batholith: Evidence for rapid mid-Cretaceous uplift and erosion within the eastern highlands of Australia. *Australian Journal of Earth Sciences* **42**, 597-607.

RADKE F. 1973 Fission-Track dating. Progress Report. (unpubl.): Amdel Project.

REINERS P. W., SPELL T. L., NICOLESCU S. & ZANETTI K. A. 2004. Zircon (U-Th)/He thermochronometry: He diffusion and comparisons with 40Ar/39Ar dating. *Geochimica et Cosmochimica Acta* **68**, 1857-1887.

REYNOLDS S. D., MILDREN S. D., HILLIS R. R. & MEYER J. J. 2006. Constraining stress magnitudes using petroleum exploration data in the Cooper–Eromanga Basins, Australia. *Tectonophysics* **415**, 123–140.

ROGERS P. & FREEMAN P. 1994 Explanatory Notes for the Warrina 1 : 250 000 Geological Map. Report Book. South Australian Department of Mines and Energy.

STUMP E. & FITZGERALD P. G. 1992. Episodic uplift of the Transantarctic Mountains. *Geology* **20**, 161-164.

TWIDALE C. R. 1994. Gondwanan (Late Jurassic and Cretaceous) palaeosurfaces of the Australian craton. *Palaeogeography, Palaeoclimatology, Palaeoecology* **112**, 157-186.

VERMEESCH P. 2009. RadialPlotter: a Java application for fission track, luminescence and other radial plots. *Radiation Measurements* **44**, 409-410.

WACLAWIK V. G., LANG S. C. & KRAPF C. B. E. 2008. Fluvial response to tectonic activity in an intra-continental dryland setting: The Neales River, Lake Eyre, Central Australia. *Geomorphology* **102**, 179-188.

WEISHEIT A., BONS P. D., DANISÍK M. & ELBURG M. A. 2014. Crustal-scale folding: Palaeozoic deformation of the Mt Painter Inlier, South Australia. *Geological Society, London, Special Publications* **394**, 53-77.

WOPFNER H. 1964. Permain-Jurassic history of the western Great Artesian Basin. *Transactions of the Royal Society of South Australia* **88**, 117-128.

WOPFNER H. 1968. Cretaceous sediments on the Mount Margaret Plateau and Evidence for Neo-Tectonism. *Quarterly Geological Notes, Geological Survey of South Australia* **28**, 7-11.

WOPFNER H. 1970. Permian paleogeography and depositional environment of the Arckaringa Basin, South Australia. *In* Proceedings and Papers IUGS Sub-Commission on Gondwana stratigraphy and palaeontology. *Second Gondwana symposium.* Council for Scientific and Industrial Research, Scientia, South Africa, 273-291.

WÜLSER P. A. 2009. Uranium metallogeny in North Flinders Ranges region of South Australia. PhD thesis. Adelaide University, Adelaide.

APPENDIX A: EXTENDED METHODOLOGY

Samples

Eight granitoid rock samples were collected from the Peake and Denison Ranges during the 1980s by University of Adelaide PhD candidate Morrison (1989) and were stored in the in the crypts at Adelaide University until selected for this Thesis. Samples 9594 (Monzonite), 9582 (Monzonite), 9528 (Monzonite), 9508 (Albitized Monzonite), 7582 (Syenite), 7571 (Syenite), and 7327 (Biotite Lamprophyre) were collected by Morrison (1989). Two apatite and zircon separates (Samples 2017960 (shortened to sample 60) which is from the Tidnamurka Rhyolite and 2017962 (shortened to sample 62) which is from the Wirriecurrie Granite) were prepared and collected from two different whole rock samples by DMITRE (Fanning *et al*. 2007). All Samples are shown in figure 2.

Crushing

The rock samples were crushed from whole rock down to a suitable grain size for separation and mounting. The first step in this process was to cut the rocks into small sizes using a Diamond Saw. These cut rocks were crushed using a Large Jaw Crusher and subsequently milled using a Ring Mill. This milled rock was sieved using a Sieve Shaker to separate the grains into three sizes >425 µm, 425-79 µm, and <79 µm. The Ring Mill and Sieve Shaker process was repeated on most of the >425 µm grains to increase the amount of 425-79 µm grains. The 425-79 µm sieved grains are optimal for this study and therefore all material in this interval were selected for mineral separation.

Mineral Separation

The sieved minerals were panned in water to remove a large majority of the lighter minerals to decrease the amount of minerals which proceeded through the Frantz Isodynamic Separator (Frantz) and Heavy Liquid Separation. All of the panned light minerals were dried in a low temperature oven (<70 °C) and kept for possible future use. The remaining minerals were heated on a low temperature hot plate (50 °C) and once dried a magnet was used to remove all the highly magnetic minerals. These magnetic minerals were saved for possible use later. The left over minerals were put through the Frantz to remove the residual magnetic minerals. The first run through was on 0.5 Amperes before the minerals which were not moved by the magnet were recycled through the Frantz at 1.4 Amperes. The magnetic minerals were kept separately for potential future use. The minerals which passed through both runs in the Frantz were separated, based on density, using the heavy liquid Methylene Iodide (which has a density of 3.3 g mL−1). The grains which sank to the bottom of this heavy liquid were collected and rinsed out with acetone to remove all traces of the heavy liquid from them. The grains which did not sink to the bottom were also collected and rinsed with acetone. They were kept for potential future use.

Picking

Apatite grains from the bottom of the heavy liquid were picked using a picking needle under two Olympus SZ61 picking microscopes. The first microscope contained a clear dish with loose grains and the second dish contained a glass slide with double sided tape on it. Underneath the glass slide, another glass slide is placed, with a '+' drawn on it 20 mm from the end and 7.5 mm in from the side. This slide acts as a guide for the location where the apatite grains will be placed on the double sided tape once the two slides are lined up correctly. Inclusion-free apatite grains with euhedral to subhedral grain shape were picked and placed in a raster on the double sided tape. Rasters of at least 12 x 12 grains were preferable, however, in cases were apatite was not abundant, smaller square rasters were used.
Five glass slides were used in total with two samples on each slide, both samples place at the same end, in line with each other 7.5 mm from the end.

Mounting, Grinding and Polishing

Mounting of the grains is required to ease the process of counting and to ensure the grains are not lost during the LA-ICP-MS sessions. Before mounting can occur, glass slides have to be placed in an array. The array is as follows: the glass slide with the apatite raster in the centre, at each end, one slide perpendicular to the end of the apatite slide, one more slide at each end on top of the slides, perpendicular with the apatite slide and about 1 cm onto the end of the apatite slide. Once the resin is placed on the apatite slide, a final slide is laid on top of the array directly on top of the apatite slide, this ensures there is one slide length between these two slides. The grains were mounted in a mixture of epoxyCure resin (20-8130-032) and epoxyCure hardener (20-8132-008) with a ratio of 5 : 1. 20 minutes of stirring the mixture was required to ensure it was mixed enough for it to be considered homogenous throughout. Once the mixture is homogeneous, small drops of it were placed on top of the apatite grain raster sitting on the double sided tape. The drops were big enough to cover the entire raster and must exceed one glass slide in height so the final slide in the array comes into contact and sticks to the resin.
The resin was left to harden over a period of 3-4 days before the two attached slides are separated using a razor blade. The razor blade has to slide between the double sided tape and the slide which the tape is attached to. Once it has completely removed the tape from the slide, the tape can be peeled off the resin, leaving the grains exposed at the top of the resin with the other end of the resin attached to the final slide in the array.

1. Once the tape is removed, the sample needs to be ground down to expose internal grain sections. The steps for grinding and polishing are as follows: Round the edges of the glass slide using Zinc Lapping Discs
2. Apply water to Waterproof Silicon Carbide Paper before grinding off the top layer of resin by applying equal pressure to the sample and moving the sample in a figure of eight around the wet carbide paper. Repeat this step, stopping to check the progress under a microscope constantly, until top layer of resin, all remaining tape and the top of the grains are removed. Begin with #1200 paper before using #2400 for finer grinding when grinding is nearing completion.

3. Once the samples are ground down to an adequate level, they must be polished. A Struers DP-U4 Cloth Lap with 3 µm or 1 µm polishing cloths and the associated diamond suspension polishing lubricant were used to polish the samples.
4. Polishing was completed in five minute blocks until fully polished, first on the 3 µm cloth and later on the 1 µm cloth for finer polishing. While polishing, the samples were held horizontal and were constantly rotated to apply an even polish on the sample.

Etching

Once the samples were polished, they were submerged and etched in 5 M HNO3 which was at 20 °C for 20 seconds. After the 20 seconds, they were dropped in a jug of water to dilute all remaining acid on the samples. Etching of Samples is required to enable fission tracks to be seen under the microscope by dissolving the surface of the grain, thus increasing the size of the fission tracks (Figure 8).

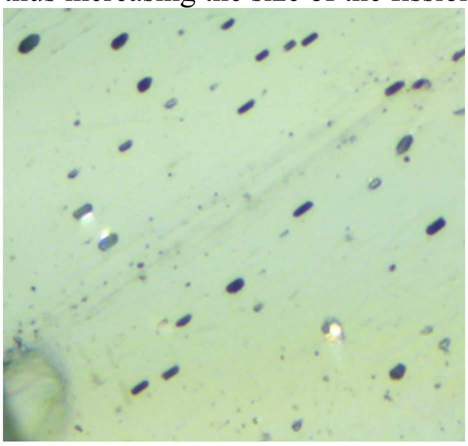

Figure 8, an example of an etched apatite grain surface. The whole are the etch pits (D_{par}) of the fission tracks. The photo is taken in reflected light using an Olympus BX51 Microscope, with an Olympus DP21 camera and computer attachment, on 100x zoom.

Counting and Measuring

Uranium is found in trace amounts within the crystal lattice in apatite and when U undergoes spontaneous fission, it damages the crystal lattice, leaving a 'fission track' (Figure 2). Each fission track is the remnant of a single fission event (Gleadow *et al.* 2002a). Above a 60 °C, these fission tracks can anneal and above 120 °C, completely repair the crystal lattice. Therefore, below 60 °C (the closure temperature), the fission tracks remain in the crystal lattice (Green *et al.* 1985). Between 60 – 120 °C (known as the partial annealing zone; PAZ), fission tracks are able to anneal but not completely repair the crystal lattice. The fission tracks anneal more (thus decreasing the length of the fission track) with more time spent within the PAZ. Shorter fission tracks indicate longer time spent within the PAZ therefore, indicating the rate of cooling. As fission tracks are only partially annealed within the PAZ, this is the temperature range which is

revealed when the AFT age is concluded when etched fission tracks are counted and combined with the U concentration of the grain.
The degree of shortening is proportional to the cooling rate and hence length measurements can be used further constrain the thermal history of the samples. Tracks which are completely confined within the crystal lattice, horizontal and etched through the contact with another track (Figure 10; TINT) or cleavage (TINCLE) can be measured to conclude the rate of cooling (Gleadow *et al*. 1986).

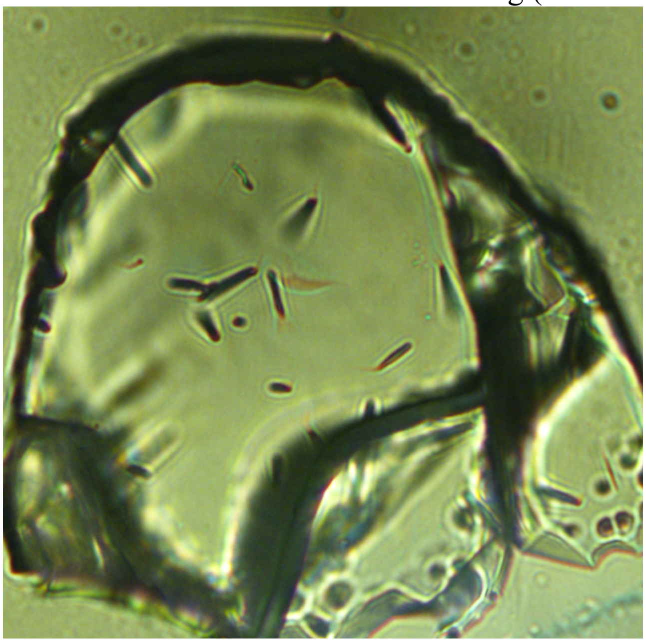

Figure 9, an example of an etched apatite grain. The dark lines within the grain are the fission tracks. The photo is taken using transmitted light on an Olympus BX51 Microscope, with an Olympus DP21 camera and computer attachment, on 100x zoom.

All counting and measuring was conducted on an Olympus BX51 Microscope, with an Olympus DP21 camera and computer attachment, on 100x zoom, using both transmitted and reflected light.
Counting was undertaken with the intention of counting 1000 fission tracks over 20-30 grains counted per sample.
Grains were selected for counting by passing a set of criteria:

1. Large enough grain size to count.
2. Random spread of fission tracks.
3. Reasonable amount of tracks, therefore, grains with too few or too many tracks were not counted.
4. Well-polished grains

Once a grain was selected for counting, the raster in the eye-piece was placed over the region of the grain to be counted and the dimensions of the counted area were documented. All the fission tracks were counted in the region and the final number was documented. A photograph was taken of the region for verification later. This process was repeated on all the grains possible until the goal number was reached.
The goal number for measuring was 100 confined tracks per sample, with a minimum of 20 confined tracks if only less than 20 confined tracks could be measured, these data was not used in further interpretations. All possible grains were checked for confined tracks and if the track could be verified to be horizontal and completely confined, its

length was measured. The angle to the C-axis and 5 D_{par} (etch pit lengths) were also measured. Finally, the type of track-intersection (TINT or TINCLE) was noted. This was repeated on each sample until all the confined tracks had been measured, limited to 100 per sample.

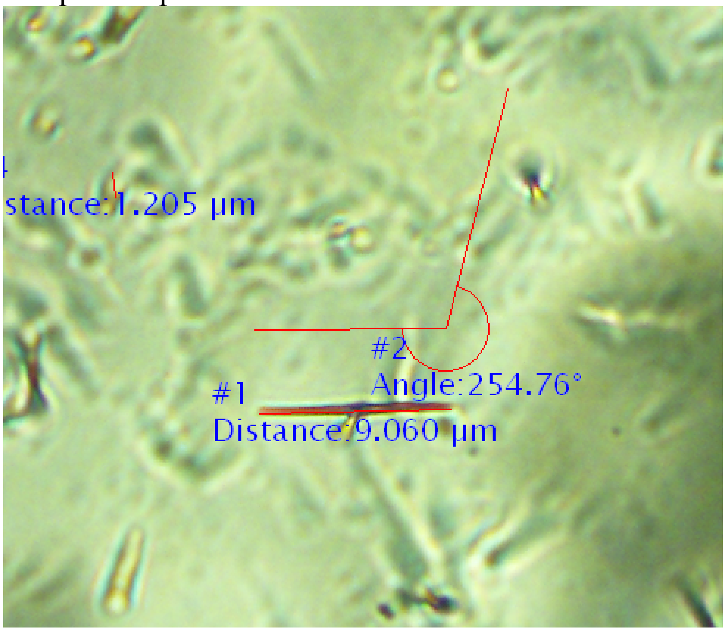

Figure 10, an example of a confined track (a TINT in this example), as indicated by the red line covering the confined track. #1 distance indicates the length and location of the track, #2 indicates the angle of the track to the C-axis of the grain wile the last measurement indicates the length of an etch pit (D_{par}; measured in reflected light). The photo is taken using transmitted light on an Olympus BX51 Microscope, with an Olympus DP21 camera and computer attachment, on 100x zoom.

LA-ICP-MS

The Laser-Ablation Inductively-Coupled-Plasma Mass-Spectrometer was used to conclude the concentrations of U^{238}, U^{235}, and Ca^{44}. This information was gathered by ablating the apatite crystals at the exact position (the actual spot size, which is listed in Table 1, used was often slightly smaller than the counted region. In this case, the spot was placed in the centre of the counted area which is a valid approach if track counts appeared homogenous throughout the counted region.) which was counted as U and Ca concentrations can change over the grain (Hasebe *et al*. 2004) and allowing the Mass-Spectrometer to calculate the concentration . All information about the LA-ICP-MS used is identified in Table 4.

A total of 160 grains were sampled on the laser not including the two sets of standards, each sample was used in an exact sequence to allow for ease in the data reduction phase. One sequence consisted of 80 unknowns measurements, therefore, the sequence was run twice to accommodate the 160.

The sequence is:

1. 3 Known glass standards (NIST 610, NIST 612 and NIST 614), each measured twice
2. 2 Apatite Durango standards
3. 8 unknowns from the samples

This sequence was repeated until all 80 unknowns are measured and repeated again for the second batch of 80 unknowns.

ICPM-MS	
Brand and model	Agilent 7700s
Forward power	1300 W
Gas flows (L/min)	
Cool (Ar)	15.00
Auxiliary (Ar)	0.89
Carrier (He)	0.70
Sample (Ar)	0.93
Laser	
Type of Laser	Excimer laser
Brand and Model	Resonetics M-50-LR
Laser wavelength	193nm
Pulse duration	20 ns
Spot size	32 µm
Repetition rate	5 Hz
Energy attenuation	50%
Laser fluency	~7 J/cm^{-2}
Laser warm up (background collection)	15 s
Data acquisition parameters	
Data acquisition protocol	Time-resolved analysis
Scanned masses	235, 238, 43
Samples per peak	1
Number of scans per peak	1
Detector mode	Pulse counting
Detector deadtime	35 ns
Background collection	15 s
Ablation for age calculation	30 s
Washout	15 s
Standardisation and data reduction	
Primary standard used	NIST 610, NIST 612, NIST 614 calibration line
Secondary standard used	Durango apatite (McDowell et al. 2005)
Data reduction software used	In-house Excel® spreadsheet
ICPM-MS	
Brand and model	Agilent 7700s
Forward power	1300 W
Gas flows (L/min)	

Table 4, the parameters for LA-ICP-MS instrumental setup, data acquisition and data reduction.

(U-Th-Sm)/He Dating

Helium (^{4}He) diffusion through the radiogenic decay of Uranium and Thorium can be used to calculate the age at which rocks passed through a certain temperature as, above this closure temperature, ^{4}He can freely diffuse out of the mineral grain, however, below the closure temperature, the ^{4}He is trapped within the grain. Therefore, by determining the amount of ^{4}He to U and Th, the age of the closure temperature (The closure temperature for apatite is 45 °C and around 170 °C for zircon) can be concluded (Farley 2002).
Two apatite separates and one zircon separate were picked using a picking needle under two Olympus SZ61 picking microscopes. Only the grains with the best grain shape, Over 70 µm in diameter and without inclusions or zonation were picked. These samples were sent to the John De Laeter Center at Curtin University in Perth for (U-Th-Sm)/He Dating. For detailed methods of (U-Th)/He Dating at John De Laeter Center, refer to Li *et al.* (2014).
Upon receiving the samples, grains which best suited the criteria for analysis were selected and measured for the calculation of an alpha correction factor (Farley *et al.* 1996).

Apatite:
He was extracted from the selected grains by loading the grains into platinum micro-crucibles and heated by a 1064 nm Nd-YAG laser. The U and Th concentration was concluded using isotope dilution. The Apatite was dissolved in 7 M HNO_3 over 12 hours and the resulting concentration of U and Th was recorded and calibrated against a standard using a Mass spectrometer.
Zircon:
The zircons were loaded into Niobium microvials and the He was extracted by heating the crystals to >1200 °C by a 1064 nm Nd-YAG laser. Isotope dilution inductively coupled mass spectrometry was used to determine the concentrations U and Th. The zircons were digested in 350 µl of HF for 40 hours, at 240 °C. Following this, 200 °C, 300 µl of HCl was used on each sample for 24 hours to dissolve any remaining fluoride salts. After the 24 hour period, the U and Th concentrations were measured with a mass spectrometer.

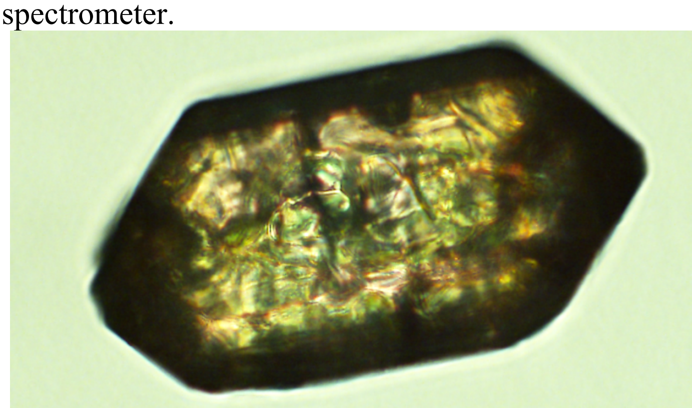

Figure 11, an example of a zircon grain used in (U-Th-Sm)/He analysis. This grain exhibits all the criteria needed for (U-Th-Sm)/He analysis. The photo is taken using transmitted light on an Olympus BX51 Microscope, with an Olympus DP21 camera and computer attachment, on 100x zoom.

APPENDIX B: EXTENDED DATA SPREADSHEETS

Durango Sample	Durango meas 238	Durango SD %	Durango meas 44	Durango SD %	Durango meas 238/44	Durango SD %	238U Dur	RF	SD	Ns	A	rho s	t (Ma)	SD t
A1 ii	5204.602	0.780542	1467202	0.797734	0.003563	0.81005	11.337	0.818022	0.092737	10	10000	100000	17.63	5.58
A1iii	5413.557	0.818547	1532061	0.715591	0.003539	0.614246	11.245	0.625923	0.070382	17	10000	170000	30.19	7.32
A1iv	5315.266	0.817117	1484304	0.762601	0.00359	0.662056	11.405	0.673017	0.076756	27	10000	270000	47.21	9.09
A1v	6183.756	0.666393	1763729	0.52731	0.003508	0.480055	11.128	0.49816	0.055435	20	10000	200000	35.87	8.02
A1vi	5786.281	0.657035	1662528	0.59703	0.003485	0.544156	11.056	0.560423	0.061961	15	10000	150000	27.10	7.00
A1vii	5967.316	0.789436	1702111	0.788077	0.003513	0.560005	11.130	0.579836	0.064535	16	10000	160000	28.71	7.18
A1viii	5959.345	0.74171	1697707	0.706684	0.003517	0.557681	11.139	0.577904	0.064373	17	10000	170000	30.47	7.39
A1ix	5890.381	0.760137	1665416	0.764708	0.003545	0.569653	11.213	0.594688	0.066683	14	10000	140000	24.94	6.67
A1x	5755.595	0.897147	1670911	0.748738	0.003448	0.636214	10.907	0.659075	0.071884	23	10000	230000	42.07	8.78
A2i	6293.804	0.794335	1303949	0.766837	0.004837	0.625549	15.278	0.654706	0.100029	11	10000	110000	14.39	4.34
A2ii	6149.711	0.731716	1286531	0.694524	0.004788	0.562224	15.121	0.594971	0.089963	19	10000	190000	25.10	5.76
A2iii	6291.256	0.821922	1296939	0.849302	0.004864	0.560383	15.339	0.600965	0.09218	17	10000	170000	22.14	5.37
A2iv	6265.231	0.719768	1307129	0.655684	0.004798	0.521549	15.132	0.565517	0.085574	28	10000	280000	36.93	6.98
A2v	5586.725	0.816144	1308790	0.767984	0.004277	0.582099	13.467	0.630377	0.084895	18	10000	180000	26.70	6.29
A2vi	5595.005	0.732748	1316169	0.661684	0.004258	0.588504	13.408	0.636897	0.085393	13	10000	130000	19.38	5.38
A2vii	7206.376	0.984337	1469407	0.962133	0.004915	0.556018	15.457	0.617001	0.095367	12	10000	120000	15.52	4.48
A2x	6258.22	0.85574	1476901	0.760441	0.004245	0.593571	13.326	0.662873	0.088337	13	10000	130000	19.50	5.41
A3 i	3976.415	0.932536	1572651	0.864427	0.002538	0.790547	8.125	0.84704	0.068823	12	10000	120000	29.49	8.52
A3 ii	4059.414	0.812417	1576875	0.453207	0.002577	0.818805	8.250	0.873551	0.072071	7	10000	70000	16.96	6.41
A3 iii	3845.016	1.003002	1547789	1.057884	0.002498	0.841842	7.995	0.89757	0.071762	9	10000	90000	22.49	7.50
A3 iv	3903.929	1.023499	1533832	0.905053	0.002548	0.710942	8.155	0.776407	0.06332	13	10000	130000	31.83	8.83
A3 v	3804.198	0.801235	1556443	0.659902	0.002449	0.724765	7.833	0.794621	0.062246	12	10000	120000	30.59	8.83
A3 vi	3860.257	1.006018	1522276	1.017043	0.002551	0.89755	8.160	0.955232	0.07795	11	10000	110000	26.92	8.12

A3 vii	3765.668	0.910583	1564796	0.660635	0.00241	0.794129	7.706	0.86646	0.066771	8	10000	80000	20.74	7.34
A3 viii	3757.928	0.853126	1558783	0.920373	0.002425	0.873483	7.755	0.940274	0.072923	10	10000	100000	25.76	8.15
A3 ix	3781.148	1.098848	1559980	0.929852	0.002429	0.783381	7.764	0.867484	0.06735	11	10000	110000	28.30	8.53
A3 x	3870.286	0.747244	1558711	0.749909	0.002491	0.709679	7.962	0.802382	0.063882	10	10000	100000	25.09	7.94
A4 i	4079.206	0.914715	1528214	0.886524	0.002681	0.791794	8.566	0.888404	0.0761	15	10000	150000	34.95	9.03
A4 ii	4155.376	0.778796	1551111	0.73691	0.002686	0.699697	8.582	0.808409	0.069374	9	10000	90000	20.96	6.99
A4 iii	4055.161	0.813519	1508372	0.864359	0.002705	0.937802	8.640	1.034416	0.089368	14	10000	140000	32.35	8.65
A4 iv	4610.728	0.933498	1497983	0.914205	0.003088	0.69177	9.863	0.819152	0.080796	22	10000	220000	44.49	9.49
A4 v	5029.624	1.056781	1535177	0.924274	0.003282	0.703321	10.480	0.847436	0.088812	22	10000	220000	41.88	8.94
A4 vi	4972.174	0.693253	1550556	0.50667	0.003212	0.71146	10.254	0.8555	0.087724	19	10000	190000	36.98	8.49
A4 vii	5109.164	0.947149	1566175	0.999849	0.003278	0.716605	10.463	0.880155	0.092087	16	10000	160000	30.54	7.64
A4 viii	4185.593	0.920435	1554199	0.822316	0.0027	0.749688	8.617	0.908676	0.078301	15	10000	150000	34.75	8.98
A4 ix	4041.448	0.922367	1491328	0.92544	0.002723	0.825923	8.687	0.992806	0.086248	17	10000	170000	39.05	9.48
A4 x	3772.82	0.80567	1438021	0.732425	0.00263	0.68756	8.390	0.882643	0.07405	18	10000	180000	42.80	10.10
A5i	15920.41	0.628208	2007784	0.588214	0.007935	0.414793	12.115	0.668396	0.080976	22	10000	220000	36.24	7.73
A5ii	16365.58	0.756642	2036690	0.73565	0.008042	0.419929	12.267	0.672414	0.082487	14	10000	140000	22.80	6.10
A5iii	15524.97	0.903861	1932048	0.908992	0.008042	0.372676	12.101	0.675033	0.081683	23	10000	230000	37.93	7.91
A5iv	15291.69	0.770835	1881252	0.728878	0.008134	0.426301	12.227	0.709104	0.086705	20	10000	200000	32.66	7.31
A5v	15248.44	0.885645	1866454	0.826312	0.008172	0.400322	12.120	0.753955	0.09138	20	10000	200000	32.94	7.37
A5vi	14747.98	0.89339	1849774	0.824401	0.007977	0.440156	11.819	0.7805	0.092251	16	10000	160000	27.04	6.76

Peake and Denison Samples

Sample	meas 238	SD %	meas 44	SD %	meas 238/44	SD %	238U Dur	RF	SD	Ns	A	rho s	t (Ma)	SD t
62 E3	4560.636	2.271577	1162135	0.992325	0.00391	1.626587	12.291	1.630588	0.200419	38	5000	760000	122.59	19.99
62 E10	4099.805	0.820335	1399297	0.708215	0.002936	0.719616	9.227	0.728657	0.067233	31	3500	885714.3	189.32	34.03
62 F6	1453.979	1.304232	1295101	0.6959	0.001121	1.002317	3.524	1.00886	0.035551	48	8100	592592.6	328.09	47.47
62 F10	3166.985	1.371508	1241485	0.913392	0.002582	1.813414	8.115	1.81706	0.147453	24	3600	666666.7	162.37	33.27
62 H5	1972.44	1.556837	1224142	0.659302	0.001606	1.188771	5.046	1.194357	0.06027	29	6000	483333.3	188.91	35.15

62 J5	1626.74	1.480605	1452648	0.914924	0.00112	1.194437	3.520	1.200072	0.042238	56	10000	560000	310.84	41.70
62 J11	4369.249	1.959497	1362536	0.649889	0.0032	1.727646	10.050	1.731576	0.174031	61	6300	968254	189.99	24.55
62K3	3490.449	1.857228	1192789	1.501114	0.002756	6.810838	8.648	6.811936	0.589073	79	5600	1410714	318.51	41.89
62 K4	2989.634	1.132928	1225262	0.852278	0.002442	0.821665	7.662	0.830822	0.06366	54	3500	1542857	390.92	53.30
62 K7	9194.591	0.924063	1683867	1.000017	0.005477	1.043609	17.182	1.051007	0.180585	107	5600	1910714	218.82	21.28
62 K8	1550.546	1.161732	1483788	0.800096	0.001047	1.013037	3.284	1.020751	0.033523	41	5400	759259.3	446.88	69.94
62 K10	2608.132	0.902472	1527272	0.911159	0.001717	0.987881	5.386	0.995889	0.053636	31	3600	861111.1	312.32	56.18
62 L1	666.1241	1.854583	999556.9	1.516241	0.000671	1.524113	2.101	1.53017	0.03215	32	6300	507936.5	466.56	82.79
62 L4	8052.788	1.125399	1187136	1.096521	0.006793	0.55166	21.285	0.568425	0.120989	171	6000	2850000	262.57	20.13
62 L5	3513.173	1.525437	1362539	0.77205	0.002574	1.2036	8.066	1.211493	0.097717	64	3500	1828571	438.50	55.07
62 L6	2957.678	1.258028	1383439	0.994108	0.002138	0.814443	6.699	0.826238	0.055351	75	6000	1250000	363.05	42.03
62 L8	3310.316	2.55634	1456060	1.205047	0.002249	1.712146	7.046	1.717962	0.121039	45	2800	1607143	441.12	66.19
62 L10	5797.034	2.357843	1498392	1.055299	0.003824	1.557203	11.977	1.563695	0.18728	70	7200	972222.2	160.46	19.34
62 L11	6914.565	0.71564	1376349	1.028215	0.005057	1.073971	15.823	1.084779	0.171644	59	3000	1966667	244.09	31.89
60 A1	2133.497	1.669652	731241.4	2.055911	0.003097	3.073669	9.691	3.077523	0.298242	36	2800	1285714	260.22	44.10
60 B1	1527.216	1.775659	978814.2	1.359928	0.001561	1.1368	4.881	1.147859	0.05603	38	4800	791666.7	316.70	51.50
60 B4	1735.939	1.120001	1231321	0.803822	0.001411	0.888237	4.413	0.902572	0.039832	87	7200	1208333	525.97	56.59
60 B9	1094.241	3.03939	741508.8	1.576035	0.001507	3.096163	4.710	3.101017	0.146052	36	3600	1000000	411.54	69.77
60 C1	1221.833	1.89824	937127.2	1.418789	0.001303	1.110111	4.070	1.123791	0.045734	23	2000	1150000	542.14	113.21
60 C3	1509.816	1.134412	1062543	1.131668	0.001431	1.083745	4.470	1.097973	0.049084	46	4000	1150000	495.35	73.24
60 C4	706.0073	3.648509	860080.7	1.951166	0.000807	2.803254	2.520	2.808872	0.07078	25	3000	833333.3	630.08	127.25
60 C9	1119.114	1.440917	1173454	1.045397	0.000955	1.098403	2.983	1.112886	0.033196	35	6000	583333.3	379.99	64.37
60 C10	3491.765	1.752334	946145.1	0.852679	0.003674	1.212352	11.475	1.225694	0.140648	82	4500	1822222	310.25	34.47
60 C11	4827.181	4.329665	869057.8	1.336932	0.005847	4.995099	18.259	4.998405	0.91267	50	1500	3333333	355.41	53.31
60 D3	3379.681	1.090632	898223.8	0.970293	0.003782	1.030704	11.799	1.049198	0.123798	36	2100	1714286	284.42	47.50
60 D6	3064.283	3.891064	1190555	0.996718	0.002507	2.906402	7.821	2.913211	0.227835	50	3000	1666667	413.02	59.64
60 D9	3519.238	4.969181	952604.1	1.775882	0.003659	4.107816	11.413	4.112708	0.469401	21	1800	1166667	201.41	44.73
60 D11	1305.025	1.596954	1016452	0.7783	0.001281	1.267013	3.994	1.283019	0.05125	46	5000	920000	445.24	65.90

7327 A1	641.1482	1.651866	1150786	0.852171	0.000559	1.538308	1.742	1.551711	0.027038	45	3500	1285714	1329.74	199.30
7327 A4	764.7456	2.388045	1145288	1.132232	0.000661	1.634896	2.061	1.647699	0.033961	42	3200	1312500	1163.02	180.48
7327 B1	643.1342	1.634777	1124749	0.720064	0.000572	1.516241	1.785	1.530238	0.02731	61	3600	1694444	1665.36	214.75
7327 B2	735.6445	1.628348	1238301	0.926835	0.000594	1.318854	1.850	1.337102	0.024733	19	5400	351851.9	369.90	85.01
7327 B9	719.0018	1.428128	1330457	0.584252	0.000542	1.511881	1.688	1.528048	0.025797	32	5000	640000	717.33	127.28
7327 B11	683.3858	1.547341	1206013	0.76367	0.000569	1.594541	1.772	1.610091	0.028531	76	4900	1551020	1549.74	179.51
7327 C1	603.2671	1.399523	1206935	0.722139	0.000501	1.272633	1.559	1.29233	0.020146	30	4200	714285.7	857.46	156.94
7327 C2	5232.883	0.921886	1196703	1.084642	0.004401	0.864436	13.707	0.893571	0.122482	215	5400	3981481	556.64	38.29
7327 C3	672.9417	1.659353	1339985	0.728724	0.000502	1.42518	1.563	1.443281	0.022554	34	5400	629629.6	759.84	130.77
7327 C7	485.1043	1.99381	1357638	1.12058	0.000361	2.417186	1.124	2.428049	0.027287	40	4000	1000000	1572.54	251.55
7327 C8	654.6547	1.391703	1251534	0.543428	0.000523	1.273036	1.629	1.29382	0.021073	46	10000	460000	541.84	80.20
7327 C11	740.71	1.991498	1337975	1.065995	0.000551	1.377075	1.713	1.398717	0.023956	142	9000	1577778	1621.64	137.96
7327 D9	697.3518	2.313792	1351596	1.732066	0.000516	1.521251	1.604	1.541122	0.024714	70	7000	1000000	1140.91	137.49
7327 D11	752.8393	1.721723	1320943	1.292858	0.000571	1.305596	1.776	1.328991	0.023606	91	10000	910000	951.58	100.55
7327 E14	634.4335	1.830784	1238157	1.549142	0.000513	1.190094	1.597	1.216039	0.019417	35	4900	714285.7	838.37	142.08
7327 F1	734.9358	1.576159	1189276	0.763293	0.000618	1.40262	1.923	1.42498	0.027403	47	4200	1119048	1070.66	156.92
7327 F6	792.9012	1.552323	1258503	0.568831	0.00063	1.492261	1.960	1.513562	0.029667	35	6300	555555.6	543.71	92.27
7327 F12	797.3541	1.681959	1286888	1.365603	0.000621	1.103329	1.929	1.132331	0.021845	97	8000	1212500	1149.16	117.40
7327 G8	764.6105	1.455945	1229907	0.727282	0.000622	1.38509	1.935	1.40859	0.027258	66	6300	1047619	1001.56	124.09
7327 G11	792.0675	1.622633	1355458	0.981617	0.000584	1.324828	1.815	1.352198	0.024546	100	7000	1428571	1409.22	142.20
7327 H2	271.1191	2.488692	1140208	0.567135	0.000238	2.462454	0.739	2.477464	0.018303	44	4200	1047619	2351.87	359.31
7327 H3	683.3352	1.428061	1184788	0.966713	0.00058	1.426161	1.801	1.452228	0.026148	39	5600	696428.6	731.08	117.55
7327 I2	709.4202	1.672583	1142629	0.893286	0.000622	1.531599	1.932	1.556186	0.03006	50	6400	781250	762.55	108.49
7327 I13	694.6511	2.094469	1236515	1.445592	0.000562	1.537188	1.744	1.561974	0.027236	31	3600	861111.1	919.59	165.79

7327 J7	721.5096	1.243599	1246351	0.668684	0.00058	1.225515	1.801	1.256823	0.022641	39	3600	1083333	1103.56	177.25
7327 J10	3472.345	2.698878	1151332	1.986458	0.002989	1.624561	9.280	1.648583	0.152995	35	3000	1166667	246.83	41.92
7582 B6i	9621.037	1.886932	1232148	1.706211	0.007788	0.527261	24.179	0.596424	0.144208	70	2000	3500000	283.40	33.92
7582 B6ii	5231.792	2.6506	657844.5	1.240746	0.007918	2.493463	24.557	2.511055	0.61665	52	1600	3250000	259.59	36.58
7582 D4	1630.399	4.345889	313108.3	4.342209	0.005597	7.237426	17.350	7.243917	1.256817	44	1500	2933333	329.81	55.16
7571 A8	4327.874	1.660975	1619286	1.091409	0.002658	0.821051	8.407	0.875745	0.073624	38	2100	1809524	417.02	67.75
7571 B4	5990.92	1.653075	1613297	1.294732	0.003706	0.773587	11.720	0.831629	0.097465	17	1600	1062500	178.95	43.43
7571 B6	3011.361	2.167116	1539121	1.857227	0.001953	0.987101	6.176	1.033319	0.063821	11	900	1222222	384.38	115.96
7571 C3	1849.065	1.686004	1531627	1.130956	0.001208	1.238834	3.821	1.276258	0.048771	21	2000	1050000	527.75	115.36
7571 D7	1992.837	1.739758	1546675	1.117492	0.001284	1.110375	4.058	1.153585	0.046815	33	2800	1178571	556.54	97.09
7571 E3	2241.522	1.2954	1624868	0.82023	0.001379	0.933938	4.358	0.985159	0.042936	36	4500	800000	357.30	59.65
7571 E4	1710.923	1.537865	1564353	1.205311	0.001094	0.929488	3.459	0.981191	0.033936	21	2400	875000	487.45	106.48
7571 E6	1155.16	1.992196	1611064	1.117382	0.000713	1.342623	2.254	1.379106	0.031082	8	1800	444444.4	383.08	135.54
7571 G1	2737.487	2.09896	1539190	1.152522	0.001772	1.655913	5.603	1.685786	0.094452	42	3000	1400000	481.67	74.77
7571 G9	1460.249	1.236204	1333515	0.640536	0.001095	1.064411	3.461	1.11056	0.038436	26	3500	742857.1	415.89	81.69
7571 H3	2097.091	1.35848	1708285	1.273779	0.001232	0.974682	3.896	1.025155	0.039939	49	6400	765625	381.81	54.68
7571 H13	1537.573	1.472937	1732250	0.862668	0.000887	1.154181	2.804	1.197355	0.033578	24	3600	666666.7	459.07	93.87
7571 I11	1491.194	1.797604	1679196	0.736457	0.000885	1.411604	2.798	1.449762	0.040569	13	2800	464285.7	323.81	89.93
7571 I13	2059.336	1.308748	1673853	1.142638	0.001235	1.194005	3.904	1.239209	0.048374	26	5600	464285.7	233.76	45.94
9582 B2	4424.756	1.104677	1523635	0.834045	0.002908	0.987343	9.189	1.042773	0.095817	38	2800	1357143	289.04	46.98
9582 B7	5086.762	6.779086	1398441	3.274342	0.003717	6.723381	11.744	6.731809	0.790576	28	1800	1555556	259.80	52.12
9582 C9	3167.946	1.609099	1726481	0.827141	0.001825	0.967684	5.764	1.030469	0.059398	11	1600	687500	234.41	70.72
9582 E9	3197.811	1.368685	1568443	0.784116	0.002033	0.903657	6.423	0.97176	0.062421	34	3000	1133333	343.80	59.06
9582 F4	846.348	2.025972	501431	1.067563	0.001678	1.436614	5.301	1.480792	0.078498	13	1200	1083333	396.57	110.15
9582 H5	2689.245	2.146032	1757038	1.373636	0.001532	1.849057	4.838	1.888037	0.091345	24	2400	1000000	400.96	82.20

9582 H9	1601.472	1.611429	1444261	1.573929	0.001115	1.046687	3.522	1.114741	0.039257	17	2000	850000	465.84	113.10
9582 I9	1628.911	1.526905	1480268	1.630051	0.00111	1.020248	3.504	1.091283	0.038234	21	2500	840000	462.85	101.13
9508 I1	2717.164	1.502236	1226578	1.236586	0.002225	1.311353	7.019	1.387091	0.097366	21	1200	1750000	480.62	105.09
9508 K3	4928.806	1.079019	1219999	1.15172	0.004058	0.760417	12.802	0.886977	0.113549	43	1600	2687500	407.05	62.18
9508 K7	3616.07	4.208095	1293922	0.80415	0.002769	4.356702	8.734	4.38304	0.382828	35	1800	1944444	430.85	75.24
9508 L3	4006.267	5.262623	1111364	1.536045	0.00367	6.271926	11.576	6.29043	0.728165	48	2000	2400000	402.16	63.32
9508 L7	4874.875	6.530091	1524165	2.220935	0.003215	5.945171	10.141	5.965074	0.604911	23	1200	1916667	367.61	79.73
9528 C2i	10009.55	0.755364	1285309	0.77884	0.007798	0.420256	24.593	0.646796	0.159069	56	2100	2666667	213.45	28.56
9528 C7	1871.6	3.170382	1150674	1.69598	0.001672	3.202025	5.271	3.243325	0.170972	24	2400	1000000	368.92	76.25
9528 C9	3853.822	2.373746	1319049	0.844022	0.002891	1.740109	9.115	1.815686	0.165492	32	2400	1333333	286.34	50.88
9528 H6	1072.422	1.53266	942865.9	0.686136	0.001141	1.512199	3.597	1.599389	0.057531	13	1800	722222.2	389.83	108.30
9528 B9	1385.955	1.932714	1416331	0.733388	0.000981	1.997034	3.091	2.065098	0.063842	13	2000	650000	407.66	113.38
9528 D7	2112.449	2.726943	1359231	0.885922	0.001587	4.134767	5.004	4.168381	0.208594	5	600	833333.3	324.97	145.96
9528 D12	2547.572	1.257807	1282671	1.033168	0.001995	1.051816	6.289	1.18973	0.074828	10	1000	1000000	310.62	98.30
9528 E7	3730.686	1.313205	1347070	0.907328	0.00277	0.945556	8.729	1.098207	0.095868	8	1200	666666.7	151.07	53.44
9528 E8	1236.359	6.750139	834086.2	5.056046	0.001396	4.113922	4.400	4.152011	0.182682	9	800	1125000	492.47	165.42
9528 J1	12463.43	0.66956	1410849	0.68328	0.008847	0.479153	27.883	0.739801	0.206279	45	2100	2142857	152.01	22.69
9528 A5	2883.103	0.966916	1139018	0.965598	0.002549	1.013561	8.033	1.160999	0.093261	11	900	1222222	297.56	89.78
9528 A7	3498.464	1.446599	1081197	0.823906	0.00323	1.035487	10.179	1.181423	0.120259	15	1400	1071429	207.30	53.58
9528 A9	2362.767	0.905161	1270471	0.915007	0.001871	0.983294	5.897	1.137245	0.067059	11	1200	916666.7	303.87	91.69
9528 C2ii	4736.808	0.805128	1230311	0.794807	0.003865	0.795262	12.179	0.98074	0.119446	41	2100	1952381	313.12	49.00
9594 A5	6569.372	3.961072	4267244	3.668744	0.001511	1.275499	5.068	1.28255	0.064995	34	3000	1133333	432.76	74.43
9594 A8	4463.201	1.144799	5315174	0.802296	0.000843	1.255897	2.827	1.263194	0.035714	20	1800	1111111	742.16	166.22
9594 B6	8383.366	2.317888	5253862	1.845547	0.001599	1.580501	5.363	1.586426	0.085077	25	2400	1041667	377.50	75.74
9594 B7	5054.786	2.676408	4959096	1.008638	0.001004	1.801795	3.366	1.80711	0.06083	14	1600	875000	500.34	134.03
9594 B11	8030.189	2.301747	5423406	1.562929	0.001471	1.226818	4.935	1.234794	0.060934	28	2100	1333333	519.30	98.35

9594 C1	9767.616	1.094529	6077608	0.817702	0.001607	0.742467	5.393	0.755896	0.040765	31	2100	1476190	525.82	94.52
9594 C7	6672.928	2.819685	4661650	1.029397	0.001438	2.866746	4.825	2.870345	0.138507	29	2000	1450000	575.01	108.04
9594 D1	7484.395	1.00646	5628494	1.146257	0.001335	0.679475	4.479	0.694907	0.031126	75	5600	1339286	572.29	66.20
9594 D4	4319.064	1.633058	4887380	1.050857	0.00088	0.93114	2.958	0.946001	0.02798	22	3500	628571.4	411.91	87.91
9594 D9	7874.955	1.738755	4841183	1.104646	0.001618	0.952769	5.438	0.967776	0.052631	41	4000	1025000	366.61	57.37
9594 E9	5950.522	2.716258	4879207	2.687962	0.001227	1.265244	4.125	1.27696	0.052678	19	2400	791666.7	373.09	85.73
9594 E14	7152.455	0.910118	5596366	0.961686	0.00128	0.696959	4.304	0.718703	0.030936	7	900	777777.8	351.87	133.02
9594 F11	14327.19	1.713946	5372109	0.871008	0.002663	1.235415	8.955	1.248654	0.111822	56	5000	1120000	245.58	32.96
9594 G10	7987.619	1.495406	4813816	1.192451	0.00166	0.864661	5.583	0.884101	0.049358	23	2800	821428.6	287.96	60.10
9594 H4	11230.27	1.000791	5295635	0.867596	0.00212	0.460832	7.133	0.4975	0.035487	33	2500	1320000	360.14	62.72
9594 H5	9000.108	1.45579	4961328	1.258437	0.001812	0.562237	6.104	0.602664	0.036785	32	3000	1066667	340.61	60.25
9594 I5	4634.169	1.5534	4916769	1.420439	0.000943	0.806028	3.177	0.835636	0.026544	16	3500	457142.9	281.79	70.49
9594 I6	12390.68	0.957546	5561492	0.826401	0.002229	0.596569	7.509	0.637222	0.04785	33	1800	1833333	471.02	82.05

Table of Constants

	TRUE CaO %	TRUE Ca %	TRUE Ca ppm	True 44 Ca	True 43 Ca	
Durango	55.77	39.8	398357	8309.73	537.7821	*based on SEM measurements CaO for Durango
P&D	55.1	39.4	393571	8209.9	531.3214	

lambda D	M	Na	lambda f	density	
1.55E-10	238.0508	6.02E+23	8.46E-17	3.22	(Gleadow)

Rsp (µm)	k
0.000725	1

Reference age (McDowell 2005)

31.44	0.18

Ca uit Barbarand et al 2003